Fireside Corrosion of Boiler Materials – Effect of Co-Firing Biomass with Coal

Report No.
COAL R267
DTI/Pub
URN 04/1795

November 2004

by

C J Davis & L W Pinder

E.ON UK (formerly Powergen UK)
Power Technology Centre
Ratcliffe-on-Soar
Nottingham
NG11 0EE

Tel: 0115 936 2000
Email: Colin.Davis@EON-UK.com

The work described in this report was carried out under contract as part of the DTI Cleaner Coal Research and Development Programme. The programme is managed by Mott MacDonald Ltd. The views and judgements expressed in this report are those of the contractor and do not necessarily reflect those of the DTI or Mott MacDonald Ltd

First published 2004

POWERGEN

UNRESTRICTED

PT/03/BB1400/R
Job No: I780/I778
January 2004

STP02/04 2003 : DTI CLEANER COAL TECHNOLOGY R&D PROGRAMME: THE EFFECT OF CO-FIRING BIOMASS WITH COAL ON THE FIRESIDE CORROSION OF BOILER MATERIALS

Prepared for

DR C H GREEN. STRATEGIC TECHNOLOGY MANAGER, WESTWOOD
(Under the Powergen Group Engineering R&D Programme)

by

C J Davis & L W Pinder

SUMMARY

In order to examine the corrosive effects of co-firing biomass with coal in existing subcritical and possible future (ultra) supercritical boilers, typical and potential boiler tube alloys have been exposed to simulated furnace wall and superheater/reheater environments in the $1MW_{TH}$ pulverised coal fired Combustion Test Facility (CTF) at Power Technology. A total of four CTF runs have been completed, each of which were nominally of 50 hours duration. Up to 15 furnace wall and 16 superheater/reheater steel alloy specimens were exposed to a range of metal temperatures, with differing heat fluxes and gaseous environments, representative of pulverised coal combustion under low NO_x conditions with biomass additions. The biomass fuels were co-fired with Daw Mill coal, furnace wall corrosion specimens having previously been tested without biomass additions in this environment, providing base line corrosion data for comparison. Numerous previous tests with coals provided baseline data for superheater/reheater corrosion rates. Biomass was fired at both 20% and 10% on a thermal basis, representing proportions significantly above and close to the maximum proportions expected to be utilised in actual plant, enabling examination of concentration effects. The specimens were exposed to the combustion environment on air-cooled, precision metrology, corrosion probes.

When co-firing with wood at both 20% and 10% on a thermal basis, there was no discernable worsening of either furnace wall or superheater/reheater corrosion when compared with firing coal alone. Whilst there was no comparable data for TP316 austenitic stainless steel superheater/reheater specimens, the measured corrosion rates were substantially reduced when compared to the ferritic T22 specimens exposed at the same location

Power Technology
Powergen UK plc
Power Technology Centre
Ratcliffe-on-Soar
Nottingham NG11 0EE

T +44 (0) 115 936 2000
F +44 (0) 115 936 2711
www.powertech.co.uk

Co-firing with Cereal Co-Product (CCP), at both 20% and 10% on a thermal basis, yielded furnace corrosion rates under reducing conditions comparable with that expected when firing coal alone. Under oxidising conditions the furnace corrosion rates were modestly increased from the expected low rates normally encountered. The T22 ferritic superheater/reheater specimens also exhibited metal wastage rates slightly increased compared with those measured previously.

However, a marked increase in the corrosion was noted in the case of the austenitic TP316 samples, where localised pitting attack resulted in peak rates similar to those measured for the T22 samples. Samples of the highly corrosion resistant HR3C material exposed whilst firing 10% CCP also suffered severe localised pitting attack, with metal wastage rates similar to that for the T22 and TP316 alloys. With only 10%CCP, the hottest operating TP316 specimen did not suffer pitting damage, suggestive of a peak in corrosion dependent upon percentage CCP burnt.

The data indicate that plant operating at relatively low final steam temperatures (~540°C), employing only low chromium containing ferritic alloys, could safely operate whilst co-firing CCP or similar fuel, and expect only slight worsening of existing corrosion rates. However, plant operating at higher steam temperatures (≥ 560°C), which contains austenitic alloys, are potentially vulnerable to greatly enhanced superheater and reheater fireside corrosion attack. Such enhanced attack would lead to a marked reduction in expected tube operating lives when compared to plant firing only coal.

With only 2 biomass fuels examined it is impossible to fully identify the reasons for the changes in corrosion rates measured. However it is likely that high alkali metal contents, and specifically potassium, in some biomass materials, are particularly aggressive. Potassium in biomass tends to be bound organically and hence is very reactive. This compares with potassium in coals, which tends to be unreactive, being well bound to mineral matter.

Consideration should be given to extending the scope of this work to include other potential biomass fuels, in order to confirm the effects of the fuel composition on wastage rates and identify which fuels can be burnt safely without adversely affecting the operating life of superheater and reheater stages. Corrosion probe exposures in actual operating plant would be required to confirm whether the high wastage rates observed in the short term CTF trials are reproduced over the longer term.

Prepared by **Approved for publication**

Original master copy signed by L W Pinder, D Armstrong & p.p. M Bolton on 16 January 2004

C J Davis and L W Pinder

D Armstrong
Boiler Technology Manager

Distribution and Title Format
S Rea
STP Technical Liaison Officer

CONTENTS

Page

1 INTRODUCTION

With the current environmental pressures to reduce the net carbon dioxide emission to atmosphere from power plant, the co-firing of non-fossil fuels such as biomass is seen as an effective way of delivering targets. Biomass is regarded as effectively a zero net emitter of carbon dioxide, only releasing recently fixed carbon when combusted. Co-firing biomass in existing boilers is seen as a potential low cost option which achieves the benefits of the high efficiencies achieved in such plant. Additional benefits may be realised by the burning of biomass in future advanced plant, designed to operate with final steam temperatures approaching 700°C, and achieving even greater efficiencies. The large scale utilisation of biomass in existing coal fired boilers is also seen as a useful way to kick start the energy from biomass industry.

Whilst many years of operational experience and testing have enabled a good understanding of fireside corrosion problems when firing coal, there remains considerable uncertainties regarding the effects of biomass additions to fuel streams. The burning of biomass on its own within power plant can often lead to severe corrosion of boiler tubing. This has resulted in restricted final steam temperatures and reduced efficiency and economic viability. The experience in dedicated biomass plant raises concerns as to the corrosive effects when co-firing.

Many potential biomass fuels are available which have widely differing properties and compositions. Plant operators primary concerns include fuel handling, performance impacts and availability of sufficient biomass to warrant undertaking plant modifications. Of the available potential fuels, wood type products and straw based products are two distinct types, are readily available in large quantities and are relatively easily handled in operational plant. As such, a single wood-based and a straw-based product were selected for testing in the current programme. The biomass fuels were co-fired with Daw Mill coal within Power Technology's 1MW Combustion Test Facility (CTF). Biomass additions were made at 20% and 10% of the total fuel flow on a thermal basis. 20% biomass was chosen in order to ensure any minor effects could be discerned, whilst 10% represented the highest levels likely to be fired in actual plant.

Sample boiler tube materials have been exposed using air cooled, precision metrology furnace wall and superheater/reheater fireside corrosion probes. Post exposure measurement and analysis has been used to determine fireside corrosion losses and mechanisms. The results of the testing have been compared with previous work firing coal without biomass in order to determine whether the biomass additions adversely affect the boiler tubing fireside corrosion performance.

2. Experimental Program

2.1 Materials

The alloys selected for testing comprised those commonly used in current subcritical coal fired plant and the most likely candidates to be employed in future (ultra) supercritical plant. Sample exposure conditions, particularly metal temperatures, were chosen as being representative of the conditions likely to be encountered in plant during normal and upset conditions.
The compositions of the furnace wall alloys in the test programme are shown in Table 1. Plain carbon steel is typically used for furnace walls in the majority of subcritical boilers. HCM2S (2%Cr), E911 (9%Cr) and HCM12 (12%Cr) represent the new family of tungsten-strengthened, chromium containing steels being considered for furnace wall tubing in ultra-supercritical plant. The latter contain extensive minor alloying additions to optimise their mechanical properties, together with additions of chromium for enhanced corrosion resistance.

The superheater/reheater alloys tested are listed in Table 2. T22 represents a commonly used material in current subcritical plant. A substantial quantity of coal-fired rig data is also available for comparison with the current programme. TP316 is also commonly used in subcritical coal fired plant with final steam temperatures of 560°C, and could be used in the early stages of superheat/reheat in advanced plant. HR3C is an alloy currently used to combat high corrosion rates in subcritical plant where alloys such as TP316 show limited operating lives, and is a potential candidate material for final superheaters and reheaters in advanced plant.

Previous short term testing within the CTF has been restricted to T22 steels. Exposure of austenitic materials was not considered appropriate as extended initiation periods of up to several thousand hours are normally considered to be required to initiate true high temperature fireside corrosion, as opposed to simple oxidation. With the requirement to consider potential (ultra) supercritical plant conditions, it was necessary to include austenitic specimens.

2.2 Exposure Conditions

Exposure of the test alloys to simulated corrosion environments was carried out in the $1MW_{Thermal}$ pulverised coal fired Combustion Test Facility (CTF) at Power Technology.

The CTF was purpose designed to recreate real plant conditions and provide a low cost combustion-testing environment. The furnace shape gives aerodynamic patterns typical of power generation boilers,

reproducing near-burner flame conditions and giving realistic in-furnace residence times. It is equipped with a comprehensive array of ports on the walls of both the furnace chamber (Figure 1) and convective duct (Figure 2). Overall, the CTF affords near-laboratory control over a range of environmental parameters representative of full-scale plant, many of which have been absent from previous laboratory based studies of fireside corrosion.

A total of 4 CTF runs were carried out, each of nominally 50 hours duration. Tests included the exposure of up to 15 furnace wall specimens and, or, 16 superheater specimens, of the various alloys. Daw Mill Coal was employed in all tests to enable comparison with previous work where this fuel was fired without the addition of biomass. Wood was co-fired using a separate feed system for the biomass, with the coal mixing prior to entering the burner. The straw based Cereal Co-Product (CCP) was co-milled with the coal and fed to the burner as a single fuel stream. The analysis for the individual and mixed fuels is given in Table 3. The CTF was operated at a total load of 0.8MW in all tests.

The specimens were carried into the combustion environment on the front face of air-cooled, precision metrology, corrosion probes (Figures 3 and 4). These probes were designed and proven under a previous Powergen/EPRI Tailored Collaboration Programme which was carried out to examine the influence of coal composition on corrosion rate, and a DTI cofunded, COST522 European Collaborative Programme [1,2,3]. Each furnace wall corrosion probe carries a single corrosion coupon, exposed to a specific metal temperature and environment. The utilisation of two thermocouples embedded at different depths in the specimen facilitated a determination of the absorbed heat flux of each sample from the measured temperature gradient. Further, extrapolation, of this temperature gradient forward allowed accurate determination and control of the front face (corrosion) temperature. The nature of the local combustion environment was characterised at two-hourly intervals throughout the exposure duration by measuring the CO and O_2 content of the furnace gas immediately adjacent to each probe.

The superheater/reheater corrosion probes typically carry 8 individual corrosion coupons of the various alloys, exposed to a range of metal temperatures and nominally the same environment. Cooling air is introduced through the centre tube to the end sample and passes along the internal surface of the samples before exhausting external to the convective pass. The cooling air is heated as it traverses the samples resulting in a temperature gradient along the length of the probe. Combustion is essentially complete when the gases and ash reach the probe(s). At this point the combustion gas contains approximately 1% O_2 and 75ppm CO

The specimens exposed, together with the individual exposure conditions are shown in Tables 4–7. Table 8 details the exposure conditions for the furnace wall specimens previously exposed whilst firing Daw Mill coal without any addition of biomass.

2.3 Ash and Corrosion Scale Characterisation

The corrosion scales and ash layers retained on the samples following exposure were characterised by optical and scanning electron microscopy (SEM), coupled with energy dispersive (EDS) and wavelength dispersive (WDS) X-ray spectroscopic analysis of the polished samples.

2.4 Measurement of Metal Loss

The short duration of the exposures requires that very accurate measurements of the metal loss be obtained. Standard methods of measuring the change in thickness of coupon samples after corrosion exposure, such as micrometer or weight loss measurements, do not posses the required accuracy. Further, utilisation of these method would have resulted in the destruction of the corrosion and ash scales, preventing their characterisation. Accordingly, metal losses were measured on polished metallographic sections using an image analysis technique, developed previously under a Powergen/EPRI Tailored Collaboration Programme. This technique retains the corrosion scales and ash layers, measures metal recession relative to a predefined surface datum, or via measurement of corrosion scale thickness, and has been proven to measure corrosion losses to an accuracy of better than ±1μm [2].

2.5 Evaluation of Alloy Performance

2.5.1 Furnace Wall Corrosion

The previous Powergen/EPRI Tailored Collaboration Programme identified that furnace wall fireside corrosion rates of plain carbon steels are dependent upon surface metal temperature, absorbed heat flux, coal chlorine content and the oxidising/reducing potential of the local combustion environment. In total, 109 specimens were exposed during 11 individual CTF runs. Even this large number of samples was insufficient to conduct a full polynomial regression analysis of the individual and interactive contributions of all of the suspected experimental variables. Nevertheless, by careful selection of exposure conditions, a satisfactory algorithm relating corrosion rate to the major variables (Equation 1) was derived and this

was validated by the successful prediction of a number of historic plant corrosion rates, both in UK and US plant [1,2].

$$M = C \times [(t_o \times K_{po})^{½} + (t_r \times K_{pr})^{½}] + [t_r \times ACR / 10^3] \quad \text{(Equation 1)}$$

Where M =Metal Loss (μm)
o & r =subscripts relating to oxidising & reducing conditions
t = Time (hours)
K_p = Parabolic Rate Constant (cm^2s^{-1})
ACR = Additional Linear Corrosion Rate (nmh^{-1})
C = Constant

The Parabolic Rate Constants under oxidising and reducing conditions are given by Equations 2 and 3, respectively.

$$K_{po} = A_o \exp-(Q_o/RT) \quad \text{(Equation 2)}$$

$$K_{pr} = A_r \times (CO)^s \times \exp-(Q_r/RT) \quad \text{(Equation 3)}$$

Where
A = Constant
Q = Activation Energy ($J.mole^{-1}$)
R = Universal Gas Constant (8.3143 $JK^{-1}mol^{-1}$)
T = Absolute Temperature (K)
CO = Percentage Carbon Monoxide in the flue gas

The Additional Linear Corrosion Rate is given by Equation 4.

$$ACR = [(N \times Cl) \times HF^n \times \exp-(Q_{Cl}/RT)]-113 \quad \text{(Equation 4)}$$

Where Cl = Percentage Coal Chlorine Content
HF = Transmitted Heat Flux (KWm^{-2})

The above work was extended to higher operating temperatures and alloy steels by the DTI / Powergen funded work conducted as part of the European COST522 project [3]. With alloy composition as an additional variable, it would have been even more impractical to attempt a full statistical analysis of the experimental data. Accordingly, the performance of each alloy was evaluated with reference to the corrosion rate predicted by Equation 1. In particular, the data were to determine whether the previously determined chlorine dependence holds at the higher anticipated metal temperatures and to estimate to what

extent the newer alloys might be more or less corrosion resistant than plain carbon steels.

Within limits, Equation 1 was found to hold true, only breaking down at higher temperatures where aggressive chlorine containing phases became unstable. Where this occurred, corrosion rates were found to be similar to that predicted for a coal containing negligible chlorine.

For the 50 hour tests in the CTF, the effect of the alloy additions were estimated according to the chromium content of the alloy and its exposure conditions. Despite the limited data available, the trends in metal loss (µm) attributable to oxidising and reducing conditions can be estimated according to Equations 5 and 6.

$$M_o = (S \times Ln\%Cr + U) \times [\, C\,(t_o \times K_{po})^{1/2}] \qquad \text{(Equation 5)}$$

$$M_r = (V \times \%Cr + W) \times [(C(t_r \times K_{pr})^{1/2}) + (t_r \times ACR / 10^3)] \qquad \text{(Equation 6)}$$

Where S, U, V & W = Constants
%Cr = Alloy Chromium Content (%)

The furnace wall samples exposed during the current programme have been compared with the predictions made above for corrosion rates when firing coal without the addition of biomass.

2.5.2 Superheater/Reheater Corrosion

The previous Powergen/EPRI Tailored Collaboration Programme included the exposure of numerous corrosion probes employing T22 specimens within the CTF. Although many different coals were burnt, the probes did not show any discernable effect of coal chemistry, rather the data was contained within a narrow scatter band, varying only with specimen metal temperature. Longer term exposures of up to 1500 hours in a 500MW coal fired boiler revealed that the wastage followed parabolic type kinetics, but that the data was still retained within the scatter band found following the CTF exposures.

The T22 samples exposed within the current test programme have been directly compared with this previous data. However no short term data is available for comparison of the austenitic alloys corrosion rates or kinetics, and hence, extrapolation of the

measured rates to long term plant operation is more difficult. The austenitic metal losses and wastage rates have been compared with those of the T22 alloy.

3. RESULTS

3.1 Wood Co-firing

3.1.1 Furnace Specimens Ash & Corrosion Scale Characterisation

All of the alloy samples exposed within the furnace section exhibited duplex corrosion scales, with the interface between the inner and outer scales representing the position of the original metal surface. Optical microscopy revealed that the samples could broadly be divided into two groups. Those exposed predominantly to oxidising conditions tended to exhibit scales that were predominantly oxides (grey) and incorporated only minor quantities of sulphides (yellow). Those samples exposed predominantly to reducing conditions incorporated a much greater proportion of sulphide, with less oxide, and were in general more defective than those exposed to oxidising conditions. In addition, the reducing samples occasionally exhibited indications of a dark phase or weeping at the metal/scale interface, indicative of the presence of chloride containing phases.

The low alloy 15Mo3 and HCM2S specimens exhibited similar scales that were often very thick, reflecting the large metal losses measured. Whilst the inner scales were often dense oxides, with finely dispersed or banded sulphides, the outer scales varied from reasonably dense oxides to very defective, predominantly sulphide scales. The samples suffered irregular general metal loss, with only minor indications of localised attack and no indication of internal attack.

The E911 and HCM12 specimens exposed to both oxidising and reducing conditions exhibited relatively thin, predominantly oxide scales, with only slight visible sulphide dispersions. Whilst the E911 samples again suffered irregular general metal losses, with the suggestion of the development of internal attack, the HCM12 specimens exhibited more localised corrosion due to limited breakdown of the existing corrosion resistant oxide.

All of the furnace samples retained particulate ash in close proximity with the corrosion scales. In addition, several samples exhibited a slight intermittent and amorphous ash layer, again in close proximity to the outer corrosion scale.

The SEM/x-ray examination confirmed the scale and ash morphologies noted optically. Typical scale and ash structures can be seen in Figures 5-6. Figure 5 shows an electron image and associated x-ray maps for the plain carbon steel specimen 6 exposed to reducing conditions whilst firing 20% wood. It can be seen that particulate ash overlays the duplex corrosion scales and that the potassium present tends to be associated with the silicate particles rather than the sulphur. The latter being associated with the corrosion scales. Figure 6 also shows the electron back scatter image and associated x-ray maps for the HCM12 specimen 10, exposed to oxidising conditions whilst firing 20% wood. Whilst particulate ash is retained on the sample, it can be seen that there is some association between the potassium and sulphur.

Elemental analysis identified that the corrosion scales comprised mixed oxides and sulphides. Alloying elements were predominantly retained within the inner scale layers with enhanced concentrations relative to the base alloy. The outer scale layers were predominantly iron oxides/sulphides with only traces of other alloying elements, and occasional contamination from the deposited ash. Chlorine was detected at levels up to a few percent close to the metal scale interface on several samples.

Elemental analysis of various layers identified can be found in Table 9. It can be seen that the condensed ash comprises predominantly sodium, sulphur and potassium, together with oxygen, and only minor concentrations of other elements. Where the condensed ash is mixed with the outer corrosion scale it is seen to contain larger proportions of iron.

3.1.2 Superheater Specimens Ash & Corrosion Scale Characterisation

Optical microscopy revealed all of the superheater/reheater alloy samples exposed within the convective section to exhibit duplex corrosion scales with only occasional indications of sulphide inclusions, again with the interface between the inner and outer scales representing the position of the original metal surface. Both the T22 and TP316 samples suffered general, irregular attack. Whilst the T22 corrosion scales were thick, reflecting the greater metal losses, the TP316 scales were frequently less than 1µm thick. Irrespective of exposure temperature or steel type the ash deposits comprised only particulate material (Figure 7).

As with the furnace wall samples, the inner corrosion scales were found to contain enhanced concentrations of alloying elements with respect to the base steel, whilst the outer corrosion scales contained only trace levels of alloying elements. The corrosion scales were predominantly oxides with only minor quantities of sulphur identified.

The elemental analysis of the various layers identified on the TP316 specimen 7 exposed whilst firing 20% wood can be found in Table 10.

3.1.3 Metal Losses

The metal losses and corresponding calculated wastage rates are shown in Tables 11-12 for both the furnace wall and superheater/reheater corrosion specimens. Table 13 details the corresponding reference furnace wall data obtained when firing Daw Mill coal without the addition of biomass. Previous CTF work and plant exposures has shown that the wastage within the furnace follows linear kinetics, hence wastage rates are reported in nmh^{-1}, as upper 95^{th} percentile, maximum and mean rates. In contrast, the previous work has shown that for the low alloy T22 steel the superheater corrosion rates follow parabolic kinetics, and hence the wastage rates are additionally reported with units cm^2s^{-1}.

3.2 Cereal Co-Product Co-firing

3.2.1 Furnace Specimens Ash & Corrosion Scale Characterisation

As with the wood co-firing tests, all of the alloy samples exposed within the furnace section exhibited duplex corrosion scales, which could again be broadly divided into two groups dependent upon whether the specimens were exposed to oxidising or reducing conditions. Of the reducing samples, those exposed whilst firing 20%CCP frequently exhibited indications of a dark phase or weeping at the metal / scale interface, again indicative of the presence of chloride containing phases, Figure 8. The reducing samples exposed whilst firing 10%CCP also occasionally exhibited evidence of chloride containing phases. The low alloy 15Mo3 and HCM2S specimens suffered irregular general metal loss and exhibited similar thick scales. The E911 and HCM12 specimens exhibited relatively thin, predominantly oxide scales.

In addition to the particulate ash that was present on all specimens, several samples exposed when firing CCP retained a condensed, or prior molten ash in intimate contact with the outer corrosion scale. Evidence for the ash having been molten took the form of precipitated iron oxide within the ash formed on solidification, Figure 9. The back scattered electron image of the HCM2S specimen exposed at 525°C to initially oxidising and subsequently reducing conditions, shows the prior molten ash as a dark layer containing multiple small crystals of lighter coloured iron oxides. The molten ash layer is in intimate contact with the outer corrosion scale. The associated x-ray maps indicate the disposition of the various elements. It can be seen that sodium, potassium and sulphur are closely associated, and, that iron from the outer corrosion scale has been incorporated within the molten ash. The aluminium and silicon associated with oxygen also indicate the presence of particulate ash derived from the coal mineral matter. The elemental analysis of various phases identified can be found in Tables 14.

3.2.2 Superheater Specimens Ash & Corrosion Scale Characterisation

On removing the superheater corrosion probe from the furnace at the end of the 20%CCP test it was noted that the radiant crown retained a white coloured ash layer underlying the surface red fly ash deposit. Where the ash was lost from the austenitic samples, the radiant crown was seen to retain a shinny, apparently undamaged metallic appearance, whilst at the 2 and 10 o'clock positions the samples were blackened and appeared pitted.

Optical microscopy revealed all of the superheater/reheater alloy samples exposed within the convective section to exhibit duplex corrosion scales, again with the interface between the inner and outer scales representing the position of the original metal surface. The T22 samples suffered general, irregular attack, resulting in thick corrosion scales, reflecting the large metal losses. Whilst much of the ash deposited on the T22 specimens was particulate in nature, there was evidence of outer scale and ash interaction, with the outer edge of the scale being mixed with agglomerating ash, Figure 10.

Much of the TP316 specimens corrosion scales were again frequently less than 1µm thick, indicative of minor corrosion having occurred. However, these specimens, and the HR3C specimens exposed during the 10%CCP trial, were found to have suffered severe localised pitting damage together with

slight internal attack. The attack was greatest at approximately the 2 and 10 o'clock positions. A typical example can be seen in Figure 11. The back scatter electron image shows a rounded pit and associated internal attack, surrounded by lesser pits and relatively unscathed surface. The associated x-ray maps indicate the fate of alloying and ash elements. It can be seen that chromium from the alloy is concentrated within the corrosion pit, but, in addition, has been drawn out into the outer corrosion scale and ash. Potassium and sulphur are closely associated within the ash deposit, and both have penetrated into the corrosion pit, although within the pit they have separated. Sulphur can also be seen to be associated with calcium beyond the area of agglomerated scale and ash. Examination of the mixed scale and ash adjacent to a similar pit at higher magnification reveals the close association of the ash and scale, the morphology of which is suggestive of precipitation of iron oxide from a prior molten ash layer, Figure 12. The elemental analysis of the various phases identified when firing CCP can be found in Table 15.

3.2.3 Metal Losses

The metal losses and corresponding calculated wastage rates are shown in Tables 16-17 for both the furnace wall and superheater/reheater corrosion specimens. Table 13 details the corresponding reference furnace wall data obtained when firing Daw Mill coal without the addition of biomass. Due to the localised nature of the attack on the austenitic superheater samples it is more appropriate to consider the upper 95th%ile metal losses and wastage rates rather than the means considered for the furnace wall samples.

4. DISCUSSION

4.1 Furnace Wall Corrosion

The ash and corrosion scales formed on the low alloy specimens exposed in the CTF were typical of those found in actual operating plant firing coal. The scales were mixed oxides and sulphides, with ash particles incorporated into the outer scale. Whilst there is little experience of 9%Cr and 12%Cr steels operating in furnace walls, it is anticipated that the corrosion scales formed would also be representative of those likely to be found in actual plant.

When firing coal alone the previous work in the CTF showed the corrosion rates to be determined by the surface metal temperature,

heat flux, alloy composition, coal chlorine content and the oxidising/reducing potential of the local environment. In particular, it was shown that under oxidising conditions low corrosion losses occurred, with rates increasing exponentially with metal temperature. Under reducing conditions, corrosion rates also increase exponentially with temperature, but in addition a synergistic effect of heat flux and coal chlorine could dramatically increase wastage rates. This additional effect operated over a limited temperature range, as at higher temperatures the formation of aggressive chloride containing phases becomes thermodynamically unfavourable. For the short 50 hour CTF tests the addition of chromium to the alloys resulted in reduced corrosion. Figures 13-16 show the comparison of each fuel for the individual alloys. Whilst the figures give no indication of the variables other than temperature and fuel type, it is possible to see that there is little difference between the losses for the Daw Mill only and the Daw Mill co-fired with wood exposures. Although variable, the data for the tests co-firing CCP often lie towards the upper bound of the scatter.

With the limited data available from the previous work, predictive equations were determined that enabled trends in metal losses to be predicted. Figure 17 shows the predicted verses actual measured corrosion losses for the samples exposed in the previous programme whilst firing Daw Mill coal without the addition of biomass. It can be seen that the general trends can be predicted with some confidence, but that the high metal losses are under predicted, whilst the low metal losses are over predicted.

When co-firing wood, the single specimen exhibiting a high metal loss is again under predicted. The bulk of the specimens experienced low metal losses (<10μm), and, as with the coal only test, were over predicted, Figure 18. When co-firing with CCP, again the highest metal losses tend to be under predicted to a similar degree, Figures 19-20. However, to some extent with 10%CCP, but more so with 20%CCP co-firing, the over prediction of lowest corrosion losses no longer occurs.

The data suggests that the greatest corrosion losses, which typically occur in plant under fault conditions with reducing environments, high heat flux (i.e. flame impingement), and with higher chlorine content coals, is unaffected by the addition of either wood or CCP to the fuel. Enhanced corrosion under these conditions continues to be due to the formation of aggressive iron or chromium chlorides at the scale metal interface.

Under normal boiler plant operating conditions, where low metal losses are expected in the presence of oxidising gases, the data suggests that the addition of wood to the fuel has no significant impact on the

expected corrosion losses. However the addition of increasing percentages of CCP to the fuel can be expected to result in modest increases in corrosion losses. The increased metal wastage occurs due to the formation of molten sulphatic phases in direct contact with the outer corrosion scale, which, in turn flux the normally protective corrosion scale, causing accelerated attack.

The greater tendency to form molten sulphatic phases when co-firing CCP is most likely due to the high levels of alkali metal present in the biomass. Unlike coals, where alkali metals such as sodium and potassium are tightly bound to mineral matter such as clays, and hence are effectively inert, in biomass these metals are found as simple salts or organic compounds, and as such, are reactive [4]. When fired, the alkali metals are released readily forming chlorides in the combustion gases. Once deposited on to the boiler tubing under oxidising conditions, they readily form sulphates [5]. The addition of SO_3 from the gases enables the formation of complex low melting point alkali trisulphates or pyrosulphates, into which the corrosion scales are fluxed.

Analysis of the material in the prior molten ash layer (Table14) revealed it to contain a range of sodium, potassium, sulphur and iron contents, suggestive of the presence of alkali pyrosulphates or alkali iron trisulphates into which the iron oxide/sulphide corrosion scale has been dissolved. Attack by molten pyrosulphates or trisulphates has been suggested as a probable mechanism of furnace wall fireside corrosion. However, there is some question as to the stability of melts in contact with the furnace walls where SO_3 does not occur at high enough concentrations to stabilise the formation of pyrosulphates [6,7].

4.2 Superheater/Reheater Corrosion

Previous testing work with a variety of UK coals in the CTF demonstrated that T22 ferritic superheater corrosion data fell within a relatively narrow range, regardless of coal composition. Indeed, the only discernable variable identified was metal temperature. The current testing of T22 steel specimens has been compared with the previous data (Figure 21). It can be seen that the data when co-firing with 20% wood lies above the expected range for firing coal alone. However, the probe exposed during the 20% wood test experienced substantial temperature variations due to variable and heavy ash deposits. As such, presenting the data as a function of mean metal temperature is misleading. When considering the cumulative exposure period within discrete temperature bands it is possible to predict the expected metal losses for the specimens using the mean and 95%ile rates. The predicted results are shown in Table 18, and it can be seen that predicted and actual metal losses correspond closely, indicating no

discernable effect for the co-firing of 20% wood. This conclusion is reinforced by the data obtained when co-firing 10% wood, which lies within the expected band bound by the previous data.

Despite the lack of data for direct comparison, Table 18 also shows that the TP316 corrosion rates determined when co-firing wood were substantially less than those measured or predicted (assuming no biomass) for the ferritic T22 steels at similar temperatures. This finding follows the expected performance of austenitic superheater/reheater materials in actual plant firing only coal.

The data obtained for the T22 specimens when co-firing CCP suggest a slight increase in wastage rates when compared with coal firing (Figure 21). This finding is consistent with the identification of scale interaction with agglomerating ash deposits in which alkali metals and sulphur were found to be associated, a feature not previously found during the 50 hour CTF runs firing coal.

Examination of the TP316 specimens after exposure when firing 20%CCP revealed the presence of severe pitting, a feature not previously found when co-firing with wood. The measured parabolic wastage rates, expressed as the upper 95%ile measurement, were seen to have increased by approximately 3 orders of magnitude when compared with the wood co-firing test. Indeed, the determined rates were of a similar order to that for the T22 specimens exposed at similar temperatures (Figure 22). This dramatic increase in rates occurred as a result of deposition of agglomerating or molten sulphate/pyrosulphate ash layers, the analysis of which can be seen in Table 15. A significant initiation period of up to several thousand hours for superheater fireside corrosion would normally be expected for austenitic stainless steels in coal fired plant. Hence, the formation of corrosion pits in excess of 50μm deep in a 50 hour CTF test was unexpected.

As a result of the TP316 pitting during the 20% CCP test, it was decided that the normally highly corrosion resistant austenitic HR3C material should be included in the experimental program for the 10%CCP test. In addition, samples of both austenitic materials would be exposed at temperatures representative of existing subcritical plant as well as (ultra) supercritical plant.

Both the TP316 and HR3C materials were found to suffer severe localised pitting damage when co-firing 10%CCP. At temperatures representative of subcritical plant the TP316 suffered wastage rates greater than that observed on the T22 specimens exposed at similar temperatures. The hottest operating TP316 specimen (690°C) however did not suffer any localised pitting attack, instead undergoing only general attack, albeit at a higher rate than observed when co-firing

wood. This finding is suggestive of a peak in corrosion pitting at a temperature dependant upon the percentage of CCP fired, or the total alkali metal in the fuel, above which corrosive attack reverts to simple oxidation. Such an effect may be due to instability of the molten ash phases at higher temperature due to dilution with a greater proportion of coal ash. To further investigate and quantify this effect would require testing with a lower percentage CCP in the fuel. Whilst the HR3C specimens also suffered severe localised pitting damage, the measured rates were slightly lower than the TP316 specimens, but still remained high, being similar to the T22 exposed whilst firing only coal.

4.3 Implications For Existing Sub-critical Plant

The data from the current test programme shows that existing subcritical plant should be able to co-fire wood based fuels with compositions similar to that tested, without encountering any significant change in existing fireside corrosion rates due to coal firing.

However, it is probable that plant firing CCP type biomass fuels with high alkali metal contents will suffer enhanced fireside corrosion. Within the furnace section, boiler plant operating at high loads or with faulty combustion equipment, leading to reducing conditions, will continue to suffer similar extreme corrosion rates due to the fuel chlorine as that found when firing only coal. Boiler plant operating with good combustion control, maintaining oxidising conditions at the furnace walls, may however also experience modest increases in fireside corrosion due to the formation of aggressive, molten sulphatic ashes.

Within the superheater/reheater stages, boilers operating with final steam temperatures of up to 540°C, in which only ferritic type T22 steels are utilised, could be expected to operate with only minor increases in fireside corrosion rates. This finding is consistent with reported operational data from utilities such as Elsam in Denmark, where commercial co-firing with straw has been undertaken on a limited basis for a number of years (8).

However, boilers currently operating with final steam temperatures of 560°C, in which extensive use of austenitic steels is made to combat existing fireside corrosion problems, are likely to be vulnerable to dramatically increased fireside corrosion. From the current data it is impossible to determine the corrosion kinetics, which in the worse case may be linear. Should such a situation prevail in actual plant, then metal losses in excess of 8mm per year are possible.

In order to determine the corrosion kinetics it would be necessary to undertake probe exposures in actual operating plant. A single probe

would be exposed for a period of 50 hours to confirm the findings of the CTF test program. In addition, a further probe would be exposed for 1000–5000 hours in order to determine whether the corrosion rates follow, for example, parabolic kinetics and decrease with time, or continue at a high rate representative of linear kinetics.

4.4 Implications For Advanced Plant

Operation of plant with advanced steam conditions demands the use of highly corrosion and creep resistant materials. The current data shows that co-firing with high percentages of biomass fuels such as wood may be possible whilst maintaining tolerable fireside corrosion performance of the superheaters and reheaters.

In contrast, co-firing with high percentages of fuels such as CCP is likely to result in unacceptably high superheater/reheater fireside corrosion rates. However, the finding that pitting did not occur on the TP316 specimen operating at the highest temperature, when co-firing 10%CCP, suggests that corrosion may be restricted with lower percentage biomass fuel content.

As with the subcritical plant, longer term testing is needed in order to confirm the corrosion kinetics, although careful selection of fuel type, based on composition, or restricting the total percentage of aggressive biomass fuels, may be sufficient to enable operation with (ultra) supercritical steam conditions.

4.5 Biomass Fuel Compositions

With testing limited to only 2 biomass fuels it is impossible to fully characterise which of the biomass components is responsible for the enhanced corrosion found. The fuel and ash analysis for the wood is suggestive of a benign fuel, and as such would not be expected to worsen fireside corrosion. Other wood products such as forestry wastes, bark, or contaminated wood may contain significant quantities of aggressive species, and as such may result in worsening of fireside corrosion rates.

The CCP contains a significantly larger ash content than the wood, and, in addition, possess a greater chlorine content. The alkali metal content (sodium and potassium) is also much greater than the wood or the Daw Mill coal. With the increases in fireside corrosion attributed to the formation of molten alkali metal sulphatic phases, it is reasonable to assume that the alkali metal content of the fuel plays a major role in determining its corrosivity.

However, it should also be noted that the CCP also contains very high levels of phosphorous, and whilst it has only been identified at relatively low levels within the ash deposits, it is possible for molten phosphates to be stable at the temperatures encountered during testing [9-12]. Despite its detection in the particulate ash layers, it is not possible to determine whether the phosphorous has played any significant role in enhancing the fireside corrosion.

Testing and operational experience in Scandinavia, with plants operating with relatively low steam temperatures and exclusively firing biomass fuels such as straw or forestry wastes, has indicated that the fuel sulphur to chlorine ratio can have a significant impact on fireside corrosion rates (13). Indeed, additives rich in sulphur have been used to reduce superheater fireside corrosion in plants exclusively firing biomass. The analysis of the CCP indicated a fuel sulphur to chlorine ratio of approximately 1.5 : 1, this being significantly lower than the value for the Daw Mill Coal (~7 : 1). Work in the United States has indicated that the fuel sulphur :2*(Max Fuel Alkali Chloride) ratio is important in determining the percentage chlorine content in ash deposits, and hence the availability of chlorine within the ash deposits to participate in corrosion. With ratios of greater than 1 : 1, i.e. at least half as much sulphur as the combined alkali metal content, sufficient sulphur exists to fully convert the alkali metal chlorides to sulphates, and, chlorides are not present in significant concentrations within the deposits [5].

5. CONCLUSIONS

5.1 The highest furnace wall fireside corrosion rates when co-firing biomass continues to be caused by the synergistic effect of fuel chlorine and heat flux under reducing conditions, the same mechanism as is responsible when firing only coal.

5.2 High percentages of wood can be co-fired without adverse corrosive effects at subcritical or (ultra) supercritical temperatures in both the furnace and superheater/reheater sections of plant.

5.3 Within the furnace section, under normal oxidising conditions, co-firing with CCP is likely to result in moderate increases to the existing low rates of fireside corrosion.

5.4 Co-firing with CCP can be expected to result in a slight increase in ferritic superheater/reheater tubing corrosion rates in comparison to plant firing only coal.

5.5 Austenitic superheater/reheater tubing can be expected to suffer a dramatic increase in fireside corrosion rates when compared with firing

coal only. Current data does not enable reliable long term wastage rate predictions, but in the worse case, with linear kinetics, metal losses in excess of 8mm per year are possible.

5.6 Careful fuel selection, or a restriction of the biomass percentage burn, would be required to enable operation of advanced plant with tolerable superheater/reheater wastage rates.

5.7 The biomass alkali metal content is implicated in the enhanced fireside corrosion process, but the current data is insufficient to permit a fully quantitative description of the aggressive components in the fuels. Fuel phosphorous or sulphur: chlorine ratios may also be important factors in determining fuel corrosivity.

6. RECOMMENDATIONS

6.1 In order to determine the exact nature of the corrosive constituents in potential biomass fuels it would be necessary to conduct further 50 hour CTF trials on fuels with differing compositions. In particular, fuels with a range of alkali metal, sulphur and chlorine contents should be examined.

6.2 A further 50 hour CTF test conducted with lower percentage CCP content would determine whether a peak in superheater/reheater corrosion rate is found at lower temperatures and characterise any dilution effect attributable to excess coal ash.

6.3 In order to better ascertain the long-term effects of co-firing fuels such as CCP on the superheater/reheater corrosion of austenitic materials in actual plant, it would be necessary to conduct short and medium term probe exposures in operating plant. Through selection of ferritic and austenitic alloy specimens, data would be relevant to sub critical plant operating with final steam temperatures of 540°C or 560°C, as well as (ultra) supercritical plant operating with advanced steam conditions.

7. REFERENCES

[1] DAVIS, C.J., JAMES, P.J. and PINDER, L.W., (2001) “Effects of Fuel Composition and Combustion Parameters on Furnace Wall Fireside Corrosion in Pulverized Coal-Fired Boilers” Materials Science Forum Vol. 369-372 (2001) pp 857-864

[2] DAVIS, C.J., JAMES, P.J. and PINDER, L.W., (2001) “Fireside Corrosion in Pulverised-Coal-Fired Boilers: Effect of Coal Chlorine and Combustion Parameters” EPRI Report 1001350, May 2001.

[3] PINDER, L.W., DAVIS, C.J., (2003), “STP 01/06 2002: COST 522: The Effect of Fuel Type on the Fireside Corrosion of Boiler Materials for Advanced Clean Coal Technologies”, PT/03/BB225/R

[4] HENDERSON, P. J., DAVIS, C., KARLSSON, A., RADEMAKERS, P., CIZNER, J., FORMANEK, B., GÖRANSSON, K., MCCOY, S. A., (2003), “In-situ Fireside Corrosion Testing Of Advanced Boiler Materials With Diverse Fuels”, Final Report From The Boiler Work Package In The COST 522 Plant Integration Group, August 2003

[5] ROBINSON, A. L., BAXTER, L. L., SCLIPPA, G., JUNKER, H., WIDELL, K. E., (1997), “Fireside Considerations When Cofiring Biomass With Coal In PC Boilers”, Engineering Foundation Conference on the Impact of Mineral Impurities in Solid Fuel Combustion, 2nd – 7th November, Keauhou Beach Hotel, Kona, Hawaii.

[6] REID, W.T., (1971), "External Corrosion and Deposits, Boiler and Gas Turbines", Fuel and Energy Science Series, American Elsevier Publishing Company Inc.

[7] DOOLEY, B. and McNAUGHTON, W., (1996),"Boiler Tube Failures: Theory and Practice, Volume 2: Water - Touched Tubes" EPRI Report TR-105261-V2

[8] OVERGAARD, P., KIRKEGAARD, N., JUNKER, H., (2002), “Experience From Large Scale Commercial Co-firing Of Biomass”, 12th European Conference on Biomass for Energy, Industry and Climate Protection, 17-21 June 2002, Amsterdam, The Netherlands.

[9] LEVIN E. M.; MCMURDIE, F.;ROBBINS, .C R.; (1964), “Phase Diagrams for Ceramists”, Figures 1-2066, Volume I, National Bureau of Standards

[10] LEVIN E. M.; MCMURDIE, F.; (1969), “Phase Diagrams for Ceramists”, Supplement Figures 2067-4149, Volume II, National Bureau of Standards

[11] LEVIN E. M.; MCMURDIE, F.; (1975), “Phase Diagrams for Ceramists”, Supplement Figures 4150-4999, Volume III, National Bureau of Standards

[12] ROTH, R. S.;NEGAS, T.;COOK, P. C.; (1987), “Phase Diagrams for Ceramists”, Supplement Figures 6255-6951, Volume VI, National Bureau of Standards

[13] HENDERSON, P., KASSMAN, H., ANDERSSON, C., (2003), “The Use of Fuel Additives In Wood And Waste Wood-Fired Boilers To Reduce

Corrosion And Fouling Problems", VGB conference, "Power Plants in Competition", Cologne, March 2003

TABLE 1: MATERIALS SELECTED FOR FURNACE WALL FIRESIDE CORROSION TESTS

Material	Nominal Composition ($^{w}/_{o}$) (Minimum and Maximum where two values given)								
	C	Si	Mn	Cr	Ni	Nb	N	Mo	Other
Plain Carbon Steel BS970 080A15	0.13 0.18		0.70 0.90						
HCM2S	0.04 0.10	0.5	0.10 0.60	1.90 2.60		0.02 0.08	0.03	0.5 3.0	B 0.006, Al 0.03, V 0.20-0.30 W 1.45-1.75
E911	0.09 0.13	0.10 0.30	0.30 0.60	8.50 9.50	0.10 0.35	0.06 0.10	0.05 0.08	0.90 1.10	Al 0.025, V 0.15-0.25, W 0.90-1.10
HCM12	0.14	0.50	0.30 0.70	11.0 13.0		0.20		0.80 1.20	V 0.20-0.30, W 0.80-1.20

TABLE 2: MATERIALS SELECTED FOR SUPERHEATER / REHEATER FIRESIDE CORROSION TESTS

Material	Nominal Composition ($^{w}/_{o}$) (Minimum and Maximum where two values given)							
	C	Si	Mn	Cr	Ni	Nb	N	Mo
T22	0.05 0.15	0.50	0.30 0.60	1.90 2.60				0.87 1.13
TP316	0.04 0.01	0.75	2.00	16.00 18.00	10.00 14.00			2.00 3.00
HR3C	0.10	1.50	2.00	23.00 27.00	17.00 23.00	0.20 0.60	0.15 0.35	

TABLE 3: FUEL ANALYSES

	DAW MILL COAL	WOOD	DAW MILL COAL + CCP BLEND (~25%)	DAW MILL COAL + CCP BLEND (~15%)	CCP
Moisture, % Total	7.0	15.3	6.2	6.5	11.8
Ash, %as received	9.0	0.4	11.8	13.3	5.3
Volatile Matter, %as received	34.0	71.4	43.0	37.5	68.9
CV, kJ/kg as received | Gross	27840	17610	24290	25090	16970
| Net	26700	16410	23160	23980	15620
Sulphur %as received	1.42	0.03	1.24	1.33	0.20
Chlorine %as received	0.20	0.03	0.22	0.25	0.13
Volatile Matter, %Dry Ash Free	40.5	84.7	52.4	46.8	83.1
CV, kJ/kg Dry Ash Free Gross	33143	20890	29622	31.284	20470
Ash Analysis					
SiO_2	49.18	43.56	46.87	51.99	1.62
Al_2O_3	26.78	3.81	20.42	20.09	0.27
Fe_2O_3	9.11	9.61	8.75	8.81	0.49
CaO	7.79	26.43	4.82	5.76	2.89
MgO	2.11	4.79	4.90	2.68	12.43

TABLE 3: FUEL ANALYSES (Continued)

	DAW MILL COAL	WOOD	DAW MILL COAL + CCP BLEND (~25%)	DAW MILL COAL + CCP BLEND (~15%)	CCP
K_2O	2.07	3.84	6.48	4.27	35.82
Na_2O	0.97	2.42	0.88	2.15	1.26
TiO_2	1.09	2.58	0.90	0.85	0.02
BaO	0.26	0.49	0.26	0.21	0.05
Mn_3O_4	0.25	1.13	0.27	0.28	0.27
P_2O_5	0.35	0.83	6.71	2.78	41.88

TABLE 4: SPECIMEN EXPOSURE CONDITIONS FOR CTF RUN 1 (80%$_{THERMAL}$ DAW MILL COAL & 20%$_{THERMAL}$ WOOD, 0.149%Cl)

Probe	CTF Port	Material	Mean O_2	Mean CO	Total Exposure	Approx. Time Oxidising	Approx. Time Reducing	Surface Metal Temp	Transmitted Heat Flux
			(%)	(%)	(Hours)	(Hours)	(Hours)	(ºC)	(KWm^{-2})
Furnace Wall Type									
1	326	E911	0.0	3.6	49.9	2.0	47.2	535	77
2	333	Carbon Steel	0.0	3.7	50.0	0.0	49.2	400	533
3	334	HCM2S	0.0	3.7	50.0	0.0	49.2	495	171
4	419	Carbon Steel	0.3	2.6	34.0	3.8	29.7	420	157
5	412	HCM2S	0.0	3.5	50.0	0.0	49.2	499	292
6	406	Carbon Steel	0.0	4.5	50.0	0.0	49.2	475	150
7	410	HCM12	0.0	3.5	50.0	0.0	49.2	525	105
8	417	E911	0.4	1.5	50.0	15.7	33.4	565	98
9	134	HCM2S	0.0	2.5	50.0	0.0	49.2	525	181
10	133	HCM12	1.6	0.8	50.0	47.8	1.3	574	92
11	124	HCM2S	3.5	0.2	50.0	49.2	0.0	524	521
12	117	HCM12	4.0	0.2	50.0	49.2	0.0	560	80
13	116	HCM12	4.0	0.2	50.1	49.2	0.0	535	67
14	115	Carbon Steel	5.1	0.1	50	49.2	0.0	420	514
15	114	Carbon Steel	6.3	0.1	50.1	49.2	0.0	400	663

TABLE 4: (Continued) SPECIMEN EXPOSURE CONDITIONS FOR CTF RUN 1 (80%$_{THERMAL}$ DAW MILL COAL & 20%$_{THERMAL}$ WOOD, 0.149%Cl)

Probe	CTF Port	Material	Mean O_2	Mean CO	Total Exposure	Approx. Time Oxidising	Approx. Time Reducing	Surface Metal Temp	Transmitted Heat Flux
			(%)	(%)	(Hours)	(Hours)	(Hours)	(ºC)	(KWm^{-2})
Superheater / Reheater Type									
16-1	526	T22	Approx.	Approx.	48.1	48.1	N/A	535	
16-2		T22	1.0	75ppm				590	
16-3		T22						637	
16-4		TP316						668	
16-5		TP316						685	
16-6		T22						694	
16-7		TP316						674	
16-8		T22						661	

TABLE 5: SPECIMEN EXPOSURE CONDITIONS FOR CTF RUN 2 (90%$_{THERMAL}$ DAW MILL COAL & 10%$_{THERMAL}$ WOOD, 0.173% Cl)

Probe	CTF Port	Material	Mean O_2	Mean CO	Total Exposure	Approx. Time Oxidising	Approx. Time Reducing	Surface Metal Temp	Transmitted Heat Flux
			(%)	(%)	(Hours)	(Hours)	(Hours)	(ºC)	(KWm^{-2})
Superheater / Reheater Type									
16-1	526	T22	Approx.	Approx.	48	48	N/A	591	
16-2		T22	1.0	75ppm				619	
16-3		T22						640	
16-4		T22						655	
16-5		T22						673	
16-6		T22						688	
16-7		T22						692	
16-8		T22						693	

TABLE 6: SPECIMEN EXPOSURE CONDITIONS FOR CTF RUN 3 (80%$_{THERMAL}$ DAW MILL COAL & 20%$_{THERMAL}$ CCP, 0.22% Cl)

Probe	CTF Port	Material	Mean O_2	Mean CO	Total Exposure	Approx. Time Oxidising	Approx. Time Reducing	Surface Metal Temp	Transmitted Heat Flux
			(%)	(%)	(Hours)	(Hours)	(Hours)	(ºC)	(KWm^{-2})
Furnace Wall Type									
1	326	E911	1.7	1.5	43.0	17.0	26.0	535	112
2	333	Carbon Steel	2.2	1.3	43.1	16.1	27.0	400	747
3	334	HCM2S	0.6	2.6	43.0	4.0	39.0	475	139
4	419	Carbon Steel	0.8	3.1	43.0	3.0	40.0	419	119
5	412	HCM2S	1.5	3.0	42.9	8.9	34.0	500	320
6	406	Carbon Steel	2.1	1.4	42.8	17.8	25.0	485	222
7	410	HCM12	0.9	2.7	42.7	5.7	37.0	524	151
8	417	E911	0.5	2.7	42.8	3.8	39.0	548	193
9	134	HCM2S	0.7	2.5	42.9	3.9	39.0	550	191
10	133	HCM12	1.5	1.0	42.8	26.8	16.0	575	69
11	124	HCM2S	3.3	0.2	42.8	42.8	0.0	524	240
12	117	HCM12	5.3	0.1	42.7	42.7	0.0	550	119
13	116	HCM12	5.9	0.1	42.7	42.7	0.0	502	78
14	115	Carbon Steel	5.8	0.1	42.7	42.7	0.0	420	264
15	114	Carbon Steel	7.1	0.0	42.7	42.7	0.0	400	174

TABLE 6: (Continued) SPECIMEN EXPOSURE CONDITIONS FOR CTF RUN 3 (80%$_{THERMAL}$ DAW MILL COAL & 20%$_{THERMAL}$ CCP, 0.22% Cl)

Probe	CTF Port	Material	Mean O_2	Mean CO	Total Exposure	Approx. Time Oxidising	Approx. Time Reducing	Surface Metal Temp	Transmitted Heat Flux
			(%)	(%)	(Hours)	(Hours)	(Hours)	(ºC)	(KWm^{-2})
Superheater / Reheater Type									
16-1	526	T22	Approx.	Approx.	42.4	42.4	N/A	515	
16-2		T22	1.0	75ppm				580	
16-3		T22						620	
16-4		TP316						658	
16-5		TP316						683	
16-6		T22						688	
16-7		TP316						693	
16-8		T22						676	

TABLE 7: SPECIMEN EXPOSURE CONDITIONS FOR CTF RUN 4 (90%$_{THERMAL}$ DAW MILL COAL & 10%$_{THERMAL}$ CCP, 0.25% Cl)

Probe	CTF Port	Material	Mean O_2	Mean CO	Total Exposure	Approx. Time Oxidising	Approx. Time Reducing	Surface Metal Temp	Transmitted Heat Flux
			(%)	(%)	(Hours)	(Hours)	(Hours)	(ºC)	(KWm^{-2})
Furnace Wall Type									
1	326	E911	0.0	4.0	48.7	0.0	47.0	525	195
2	333	Carbon Steel	1.0	1.8	48.7	13.0	33.0	400	433
3	334	HCM2S	0.0	4.1	48.7	0.0	47.0	475	264
4	419	Carbon Steel	0.0	4.1	48.4	0.0	47.0	428	488
5	412	HCM2S	0.0	4.8	48.4	0.0	47.0	500	349
6	406	Carbon Steel	1.2	2.3	48.3	12.0	23.0	450	121
7	410	HCM12	0.9	1.8	48.1	13.0	25.0	525	138
8	417	E911	0.4	1.6	48.1	13.0	26.0	550	282
9	134	HCM2S	0.9	1.2	48.1	22.0	23.0	525	48
10	133	HCM12	2.3	0.3	48.1	45.0	2.0	575	198
11	124	HCM2S	6.5	0.1	48.1	47.0	0.0	525	137
12	116	E911	9.2	0.0	47.9	47.0	0.0	550	132
13	115	Carbon Steel	8.1	0.0	48.0	47.0	0.0	424	401
14	114	Carbon Steel	9.9	0.0	47.9	47.0	0.0	400	135

TABLE 7: (Continued) SPECIMEN EXPOSURE CONDITIONS FOR CTF RUN 4 (90%$_{THERMAL}$ DAW MILL COAL & 10%$_{THERMAL}$ CCP)

Probe	CTF Port	Material	Mean O_2	Mean CO	Total Exposure	Approx. Time Oxidising	Approx. Time Reducing	Surface Metal Temp	Transmitted Heat Flux
			(%)	(%)	(Hours)	(Hours)	(Hours)	(ºC)	(KWm^{-2})
Superheater / Reheater Type									
15-1	525	T22	Approx.	Approx.	46.5	46.5	N/A	507	
15-2		HR3C	1.0	75ppm				610	
15-3		HR3C						629	
15-4		T22						655	
15-5		T22						649	
15-6		T22						666	
15-7		HR3C						669	
15-8		T22						616	
16-1	526	T22	Approx.	Approx.	47.8	47.8	N/A	478	
16-2		TP316	1.0	75ppm				598	
16-3		TP316						620	
16-4		T22						664	
16-5		T22						666	
16-6		T22						674	
16-7		TP316						690	
16-8		T22						624	

TABLE 8: SPECIMEN EXPOSURE CONDITIONS FOR REFERENCE CTF RUNS (100%$_{THERMAL}$ DAW MILL COAL, 0.18%Cl)

Probe	CTF Port	Material	Mean O_2	Mean CO	Total Exposure	Approx. Time Oxidising	Approx. Time Reducing	Surface Metal Temp	Transmitted Heat Flux
			(%)	(%)	(Hours)	(Hours)	(Hours)	(ºC)	(KWm^{-2})
Furnace Wall Type									
	326	HCM2S	0	2.8	47.12	4	43	500	44
	333	15Mo3	0.8	2	47.2	22	26	470	206
	334	HCM2S	0.2	3.6	47.2	6	42	550	66
	419	HCM2S	0	4.6	47.2	0	47	475	66
	412	HCM2S	0	3.6	47.4	1	46	525	321
	406	15Mo3	0	2.9	47.2	1	46	475	135
	410	E911	0	4.5	47.03	0	47	525	42
	417	E911	0.3	3.6	47.13	9	38	475	103
	134	E911	0	5	47.17	0	47	550	31
	133	E911	0	4.6	47.15	0	47	500	88
	116	E911	1.8	0.9	47.42	35	11	525	172
	115	HCM2S	2.6	0.4	47.15	46	1	525	123
	326	HCM12	0	2.7	47.83	2	45	500	43
	333	15Mo3	0	4.2	48.11	2	45	450	277
	334	HCM12	0.2	3.9	48.1	3	45	546	143
	419	HCM12	0.4	4	47.87	7	41	476	101
	412	HCM12	0.2	3.5	48.08	2	45	525	228
	406	15Mo3	0.2	2.3	48.08	12	36	500	50
	115	HCM12	4.2	0.2	48.03	47	0	520	157

TABLE 9: WOOD CO-FIRING ELEMENTAL ANALYSIS FOR ASH DEPOSITS ON FURNACE SAMPLES (ATOMIC %)

		O	Na	Mg	Al	Si	P	S	K	Ca	Ti	Cr	Mn	Fe	Ni	Zn	Mo	Ba	Phases Identified
Particulate Ash	Max	63	6	1	4	18		3	3	2				4			1		Alumino Silicates
	Min	50	6	1	1	17		0	2	1				2			0		
Partly Condensed	Max	56	13	1	9	18		12	6	2				6		2	2		$(Na,K)2SO_x.Fe_yO_z$, $(Na,K)S_2Ox.Fe_yO_z$
	Min	45	6	<1	1	<1		2	2	<1						0	0		Alumino Silicates
Mixed Scale/Ash	Max	48	10	1	6	8		12	5	3				7					$(Na,K)2SO_x.Fe_yO_z$
	Min																		

TABLE 10: WOOD CO-FIRING ELEMENTAL ANALYSIS FOR ASH DEPOSITS ON SUPERHEATER/REHEATER SAMPLES (ATOMIC %)

		O	Na	Mg	Al	Si	P	S	K	Ca	Ti	Cr	Mn	Fe	Ni	Zn	Mo	Ba	Phases Identified
Particulate Ash	Max	62	2	1	8	20		1	1	1				2					Alumino Silicate
	Min																		

TABLE 11: CORROSION LOSSES AND WASTAGE RATES FOR CTF RUN 1 (80%$_{THERMAL}$ DAW MILL COAL & 20%$_{THERMAL}$ WOOD)

Probe	Material	Total Measured Metal Loss			Linear Wastage Rate			Parabolic Wastage Rate		
		95%ile (μm)	Max (μm)	Mean (μm)	95%ile (nmh^{-1})	Max (nmh^{-1})	Mean (nmh^{-1})	95%ile (cm^2s^{-1})	Max (cm^2s^{-1})	Mean (cm^2s^{-1})
Furnace Wall Samples										
1	E911	13.0	15.4	10.6	261	309	212			
2	Carbon Steel	6.3	8.2	2.9	125	164	58			
3	HCM2S	22.2	26.6	7.6	444	533	152			
4	Carbon Steel	9.9	12.0	7.7	292	352	228			
5	HCM2S	70.1	73.2	56.5	1402	1465	1131			
6	Carbon Steel	6.3	6.0	4.2	125	121	84			
7	HCM12	9.2	19.8	3.6	183	395	71			
8	E911	9.7	11.4	6.0	193	227	120			
9	HCM2S	11.4	15.0	8.5	229	301	170			
10	HCM12	6.8	8.4	3.7	136	167	75			
11	HCM2S	9.6	13.4	8.2	192	268	164			
12	HCM12	6.2	7.5	3.8	124	150	76			
13	HCM12	4.6	6.1	2.8	91	122	56			
14	Carbon Steel	3.0	5.4	1.3	59	109	26			
15	Carbon Steel	3.8	6.0	2.1	75	119	42			

TABLE 11: (Continued) CORROSION LOSSES AND WASTAGE RATES FOR CTF RUN 1 (80%$_{THERMAL}$ DAW MILL COAL & 20%$_{THERMAL}$ WOOD)

Probe	Material	Total Measured Metal Loss			Linear Wastage Rate			Parabolic Wastage Rate		
		95%ile (μm)	Max (μm)	Mean (μm)	95%ile (nmh^{-1})	Max (nmh^{-1})	Mean (nmh^{-1})	95%ile (cm^2s^{-1})	Max (cm^2s^{-1})	Mean (cm^2s^{-1})
Superheater / Reheater Samples										
16-1	T22	18.4	18.4	12	383	383	249	$1.95x10^{-11}$	$1.95x10^{-11}$	$8.31x10^{-12}$
16-2	T22	32.2	34.1	18.2	669	709	378	$5.98x10^{-11}$	$6.71x10^{-11}$	$1.91x10^{-11}$
16-3	T22	51	51.2	32.4	1060	1064	674	$1.50x10^{-10}$	$1.51x10^{-10}$	$6.06x10^{-11}$
16-4	TP316	2.9	4.3	0.4	60	89	8	$4.86x10^{-13}$	$1.07x10^{-12}$	$9.24x10^{-15}$
16-5	TP316	4.8	6.8	0.5	100	141	10	$1.33x10^{-12}$	$2.67x10^{-12}$	$1.44x10^{-14}$
16-6	T22									
16-7	TP316	5.1	7	0.6	106	146	12	$1.50x10^{-12}$	$2.83x10^{-12}$	$2.08x10^{-14}$
16-8	T22	81.4	82.5	69.1	1692	1715	1437	$3.83x10^{-10}$	$3.93x10^{-10}$	$2.76x10^{-10}$

TABLE 12: CORROSION LOSSES AND WASTAGE RATES FOR CTF RUN 2 (90%$_{THERMAL}$ DAW MILL COAL & 10%$_{THERMAL}$ WOOD)

Probe	Material	Measured Metal Loss			Linear Wastage Rate			Parabolic Wastage Rate		
		95%ile (μm)	Max (μm)	Mean (μm)	95%ile (nmh^{-1})	Max (nmh^{-1})	Mean (nmh^{-1})	95%ile (cm^2s^{-1})	Max (cm^2s^{-1})	Mean (cm^2s^{-1})
Superheater / Reheater Samples										
16-1	T22	4.38	4.5	3.2	91	94	67	$1.11x10^{-12}$	$1.17x10^{-12}$	$5.93x10^{-13}$
16-2	T22	6.7	8.5	4.8	140	177	100	$2.60x10^{-12}$	$4.18x10^{-12}$	$1.33x10^{-12}$
16-3	T22	11.5	14.2	8.5	240	296	177	$7.65x10^{-12}$	$1.17x10^{-11}$	$4.18x10^{-12}$
16-4	T22	25.6	26.9	17.5	533	560	365	$3.79x10^{-11}$	$4.19x10^{-11}$	$1.77x10^{-11}$
16-5	T22	32.9	35.1	25.7	685	731	535	$6.26x10^{-11}$	$7.13x10^{-11}$	$3.82x10^{-11}$
16-6	T22	38.7	42.8	29.1	806	892	606	$8.67x10^{-11}$	$1.06x10^{-10}$	$4.9x10^{-11}$
16-7	T22	56.5	59.2	36.9	1177	1233	769	$1.85x10^{-10}$	$2.03x10^{-10}$	$7.88x10^{-11}$
16-8	T22	45.8	59.9	33.8	954	1248	704	$1.21x10^{-10}$	$2.08x10^{-10}$	$6.61x10^{-11}$

TABLE 13: CORROSION LOSSES AND WASTAGE RATES FOR REFERENCE CTF RUN (100%$_{THERMAL}$ DAW MILL COAL)

Probe	Material	Measured Metal Loss			Linear Wastage Rate			Parabolic Wastage Rate		
		95%ile (μm)	Max (μm)	Mean (μm)	95%ile (nmh^{-1})	Max (nmh^{-1})	Mean (nmh^{-1})	95%ile (cm^2s^{-1})	Max (cm^2s^{-1})	Mean (cm^2s^{-1})
Furnace Wall Samples										
	HCM2S	11.6	14.8	5.7	246	314	121			
	15Mo3	59.4	67.9	33.5	1258	1439	710			
	HCM2S	56.8	58.8	50.4	1203	1246	1068			
	HCM2S	9.3	12.0	4.7	197	254	100			
	HCM2S	85.0	88.9	65.9	1793	1876	1390			
	15Mo3	5.6	10.1	2.7	119	214	57			
	E911	6.5	8.5	4.0	138	181	85			
	E911	16.3	17.2	13.0	346	365	276			
	E911	13.9	15.0	9.7	295	318	206			
	E911	24.1	26.7	14.6	511	566	310			
	E911	6.6	11.0	3.7	139	232	78			
	HCM2S	6.8	7.8	4.7	144	165	100			
	HCM12	6.0	7.6	4.2	243	309	88			
	15Mo3	83.7	94.3	57.5	1740	1960	1195			
	HCM12	6.5	7.4	4.2	1181	1222	87			
	HCM12	4.5	7.9	2.6	194	251	54			
	HCM12	8.4	10.8	5.6	1768	1849	116			
	15Mo3	11.6	13.6	6.2	241	283	129			
	HCM12	4.8	6.2	3.1	100	129	65			

TABLE 14: CCP CO-FIRING ELEMENTAL ANALYSIS FOR ASH DEPOSITS ON FURNACE SAMPLES (ATOMIC %)

		O	Na	Mg	Al	Si	P	S	K	Ca	Ti	Cr	Mn	Fe	Ni	Zn	Mo	Ba	Phases Identified
Particulate Ash	Max	62	20	16	16	38	16	13	23	19				45		2			Alumino Silicates, Silica, $MgPO_x$, $(Mg,Ca)P_xO_y$, MP_xO_y, $(Na,K)2SO_x$, $(Na,K)3SO_x$
	Min	25	0	0	0	0	0	0	0	0				0		0			
Precipitated Oxide	Max	48	2			2		3	2					52					FeO_x
	Min	41	0			0		0	0					44					
Condensed / Prior Molten	Max	68	23	1	4	24	3	21	29	2				7			2		$(Na,K)SO_x$, $(Na,K)2SO_x$, $(Na,K)3SO_x$, $(Na,K)2SO_x.Fe_yO_z$, $(Na,K)3SO_x.Fe_yO_z$, KSO_x, $KSO_x.Fe_yO_z$, Silica
	Min	32	0	0	0	0	0	3	3	0				0			0		
Mixed Scale/Ash	Max	64	22	2	10	24	5	23	23	15	3			63					Alumino Silicates, Silica, $(Na,K)SO_x.Fe_yO_z$, $KSO_x.Fe_yO_z$, FeO_x, $CaSO_4$, $(Na,K)2SO_x.Fe_yO_z$, $(Na,K)3SO_x.Fe_yO_z$
	Min	29	0	0	0	1	0	0	1	0	0			4					

TABLE 15: CCP CO-FIRING ELEMENTAL ANALYSIS FOR ASH DEPOSITS ON SUPERHEATER/REHEATER SAMPLES (ATOMIC %)

		O	Na	Mg	Al	Si	P	S	K	Ca	Ti	Cr	Mn	Fe	Ni	Zn	Mo	Ba	Phases Identified
Particulate Ash	Max	53	4	2	11	24	1	12	5	12				4					Alumino Silicates,
	Min	49	2	0	3	8	0	2	2	1				2					$CaSO_4$
Condensed	Max	59	18	4	5	28		18	12	6			1	9	5				$(Na,K)2SO_x$, KSO_x,
	Min	34	0	2	0	1		4	4	4				1	1				$(Na,K)SO_x.Fe_yO_z$,
Mixed Scale/Ash	Max	61	16	4	7	25	2	16	11	3		6	1	40	13			15	Alumino Silicates, $(Na,K)SO_x$, $(Na,K)SO_x.Fe_yO_z$, FeO_x, NiO, CrS_x,
	Min	32	0	0	0	1	0	2	1	0		0	0	3	0			0	$BaSO_4$

TABLE 16: CORROSION LOSSES AND WASTAGE RATES FOR CTF RUN 3 (80%$_{THERMAL}$ DAW MILL COAL & 20%$_{THERMAL}$ CCP)

Probe	Material	Measured Metal Loss			Linear Wastage Rate			Parabolic Wastage Rate		
		95%ile (μm)	Max (μm)	Mean (μm)	95%ile (nmh^{-1})	Max (nmh^{-1})	Mean (nmh^{-1})	95%ile (cm^2s^{-1})	Max (cm^2s^{-1})	Mean (cm^2s^{-1})
Furnace Wall Samples										
1	E911	42.3	50.6	23.7	984	1177	551			
2	Carbon Steel	8.5	15.0	3.3	198	349	76			
3	HCM2S	30.8	38.3	16.0	716	890	372			
4	Carbon Steel	44.1	55.3	20.8	1025	1286	484			
5	HCM2S	53.2	61.9	39.1	1241	1444	912			
6	Carbon Steel	40.5	46.6	21.9	947	1090	513			
7	HCM12	29.9	40.2	18.5	700	941	432			
8	E911	68.0	81.5	41.0	1590	1904	958			
9	HCM2S	105.3	111.1	85.0	2455	2589	1981			
10	HCM12	36.1	42.2	22.8	843	985	533			
11	HCM2S	10.6	17.3	6.8	248	405	159			
12	HCM12	15.3	20.2	13.1	359	473	308			
13	HCM12	8.2	9.9	4.4	192	232	102			
14	Carbon Steel	7.6	13.1	2.9	178	306	67			
15	Carbon Steel	12.1	15.9	6.5	284	372	152			

TABLE 16: (Continued) CORROSION LOSSES AND WASTAGE RATES FOR CTF RUN 3 (80%$_{THERMAL}$ DAW MILL COAL & 20%$_{THERMAL}$ CCP)

Probe	Material	Measured Metal Loss			Linear Wastage Rate			Parabolic Wastage Rate		
		95%ile (μm)	Max (μm)	Mean (μm)	95%ile (nmh^{-1})	Max (nmh^{-1})	Mean (nmh^{-1})	95%ile (cm^2s^{-1})	Max (cm^2s^{-1})	Mean (cm^2s^{-1})
Superheater / Reheater Samples										
16-1	T22	3.5	3.5	1.7	83	83	40	$8.03x10^{-13}$	$8.03x10^{-13}$	$1.89x10^{-13}$
16-2	T22	7.3	8.6	4.6	172	203	108	$3.49x10^{-12}$	$4.85x10^{-12}$	$1.39x10^{-12}$
16-3	T22	21.8	24.3	10.6	514	573	250	$3.11x10^{-11}$	$3.87x10^{-11}$	$7.36x10^{-12}$
16-4	TP316	39	50	8.3	920	1179	196	$9.96x10^{-11}$	$1.64x10^{-10}$	$4.51x10^{-12}$
16-5	TP316	44.7	64.1	10	1054	1512	236	$1.30x10^{-10}$	$2.69x10^{-10}$	$6.55x10^{-12}$
16-6	T22	64.1	67	37.5	1512	1580	884	$2.69x10^{-10}$	$2.94x10^{-10}$	$9.21x10^{-11}$
16-7	TP316	70.1	100.3	14	1653	2366	330	$3.22x10^{-10}$	$6.59x10^{-10}$	$1.28x10^{-11}$
16-8	T22	62.5	68.7	42	1474	1620	991	$2.56x10^{-10}$	$3.09x10^{-10}$	$1.16x10^{-10}$

TABLE 17: CORROSION LOSSES AND WASTAGE RATES FOR CTF RUN 4 (90%$_{THERMAL}$ DAW MILL COAL & 10%$_{THERMAL}$ CCP)

Probe	Material	Measured Metal Loss			Linear Wastage Rate			Parabolic Wastage Rate		
		95%ile (μm)	Max (μm)	Mean (μm)	95%ile (nmh^{-1})	Max (nmh^{-1})	Mean (nmh^{-1})	95%ile (cm^2s^{-1})	Max (cm^2s^{-1})	Mean (cm^2s^{-1})
Furnace Wall Samples										
1	E911	64.5	78.0	52.8	1325	1601	1084			
2	Carbon Steel	6.0	9.1	4.0	123	187	82			
3	HCM2S	60.4	76.4	39.4	1240	1570	810			
4	Carbon Steel	63.0	69.0	44.8	1302	1426	926			
5	HCM2S	34.6	38.7	26.5	715	799	547			
6	Carbon Steel	31.7	36.0	21.8	656	745	451			
7	HCM12	32.7	79.6	13.8	679	1656	287			
8	E911	21.2	25.3	10.9	441	527	227			
9	HCM2S	78.7	93.3	34.5	1635	1940	718			
10	HCM12	8.5	12.4	2.9	177	257	61			
11	HCM2S	7.3	8.8	5.0	152	183	104			
12	E911	8.0	10.3	5.1	167	215	106			
13	Carbon Steel	4.3	5.6	1.7	90	117	35			
14	Carbon Steel	3.2	5.0	0.9	67	104	19			

TABLE 17: (Continued) CORROSION LOSSES AND WASTAGE RATES FOR CTF RUN 4 (90%$_{THERMAL}$ DAW MILL COAL & 10%$_{THERMAL}$ CCP)

Probe	Material	Measured Metal Loss			Linear Wastage Rate			Parabolic Wastage Rate		
		95%ile (μm)	Max (μm)	Mean (μm)	95%ile (nmh^{-1})	Max (nmh^{-1})	Mean (nmh^{-1})	95%ile (cm^2s^{-1})	Max (cm^2s^{-1})	Mean (cm^2s^{-1})
Superheater / Reheater Samples										
15-1	T22	Not Measured								
15-2	HR3C	6	33.4	1.3	129	718	28	$2.15x10^{-12}$	$6.66x10^{-11}$	$1.01x10^{-13}$
15-3	HR3C	29.9	39.9	3.7	643	858	80	$5.34x10^{-11}$	$9.51x10^{-11}$	$8.18x10^{-13}$
15-4	T22	Not Measured								
15-5	T22	35.83	37.2	21.23	771	800	457	$7.67x10^{-11}$	$8.27x10^{-11}$	$2.69x10^{-11}$
15-6	T22	46.28	57.3	33.13	995	1232	712	$1.28x10^{-10}$	$1.96x10^{-10}$	$6.56x10^{-11}$
15-7	HR3C	53.1	77.4	8	1142	1665	172	$1.68x10^{-10}$	$3.58x10^{-10}$	$3.82x10^{-12}$
15-8	T22	26.3	43.5	14.26	566	935	307	$4.13x10^{-11}$	$1.13x10^{-10}$	$1.21x10^{-11}$
16-1	T22	5.4	5.6	4.2	113	117	89	1.69E-12	1.82E-12	1.04E-12
16-2	316	34.0	40.8	8.5	711	854	178	6.72E-11	9.67E-11	4.20E-12
16-3	316	59.1	82.6	12.2	1236	1728	255	2.03E-10	3.96E-10	8.65E-12
16-4	T22	45.9	50.9	28.3	960	1065	593	1.26E-10	1.55E-10	4.79E-11
16-5	T22	43.5	45.8	31.3	910	958	655	1.13E-10	1.25E-10	5.86E-11
16-6	T22	Not Measured								
16-7	316	18.5	28.5	6.4	387	596	134	1.99E-11	4.72E-11	2.38E-12
16-8	T22	Not Measured								

TABLE 18: MEASURED AND PREDICTED SUPERHEATER REHEATER CORROSION LOSSES, CO-FIRING 20% WOOD

SPECIMEN	Measured Mean Metal Loss (µm)	Predicted Mean T22 Metal Loss (µm)	Measured 95%ile Metal Loss (µm)	Predicted 95%ile T22 Metal Loss (µm)	COMMENT
1	12.0	12.2	18.4	13.0	
2	18.2	-	32.2	-	Thermocouple Failed
3	32.4	23.3	51.0	30.4	
4	0.4	19.4	2.9	25.1	TP316 Austenitic Sample
5	0.5	66.6	4.8	82.8	TP316 Austenitic Sample
6	-	102.6	-	125.6	Not Measured, Scale Lost
7	0.6	73.3	5.1	91.5	TP316 Austenitic Sample
8	82.5	73.9	81.4	92.3	

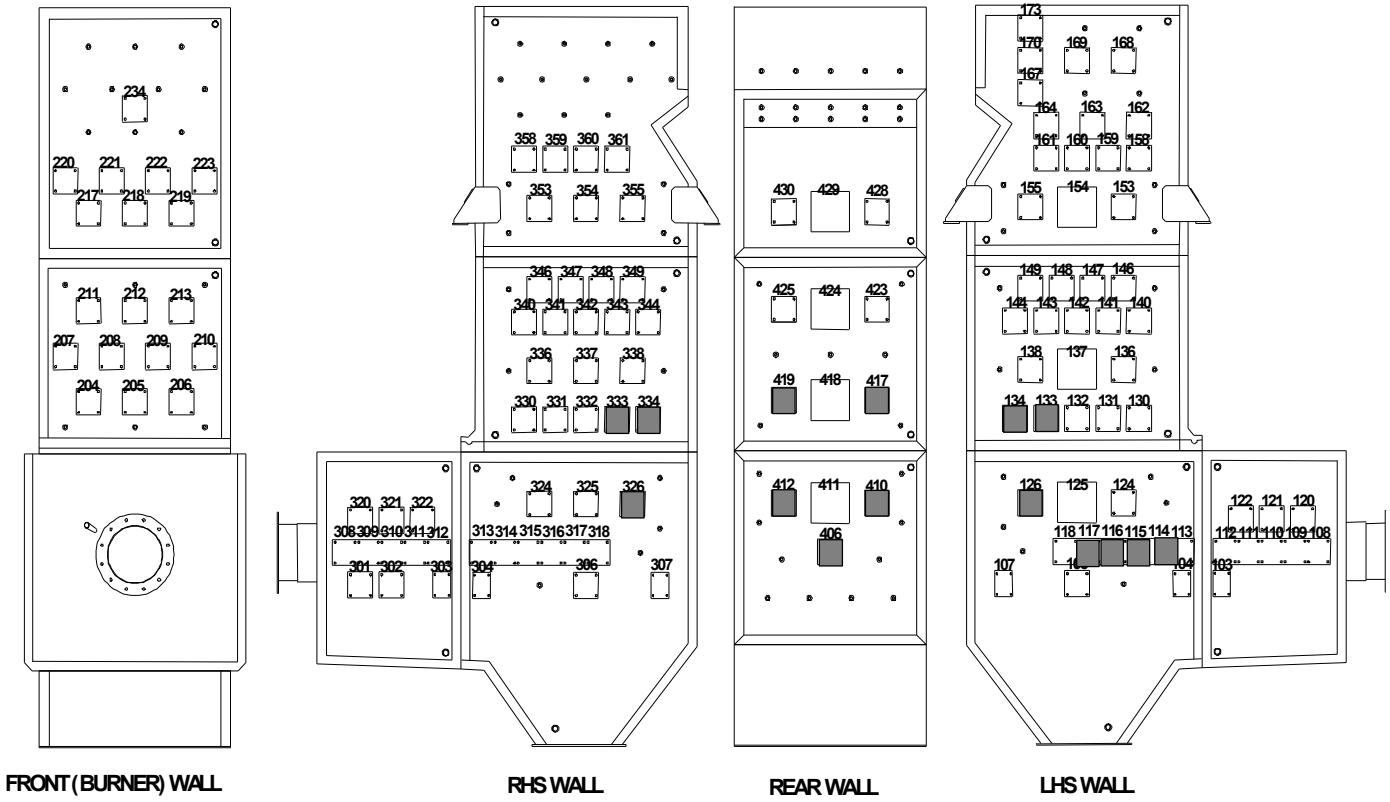

FIGURE No.1 **EXPLODED DIAGRAM OF THE COMBUSTION TEST FACILITY FURNACE SHOWING LAYOUT AND LOCATION OF SAMPLING PORTS (SHADED PORTS INDICATE POSITION OF PROBES)**

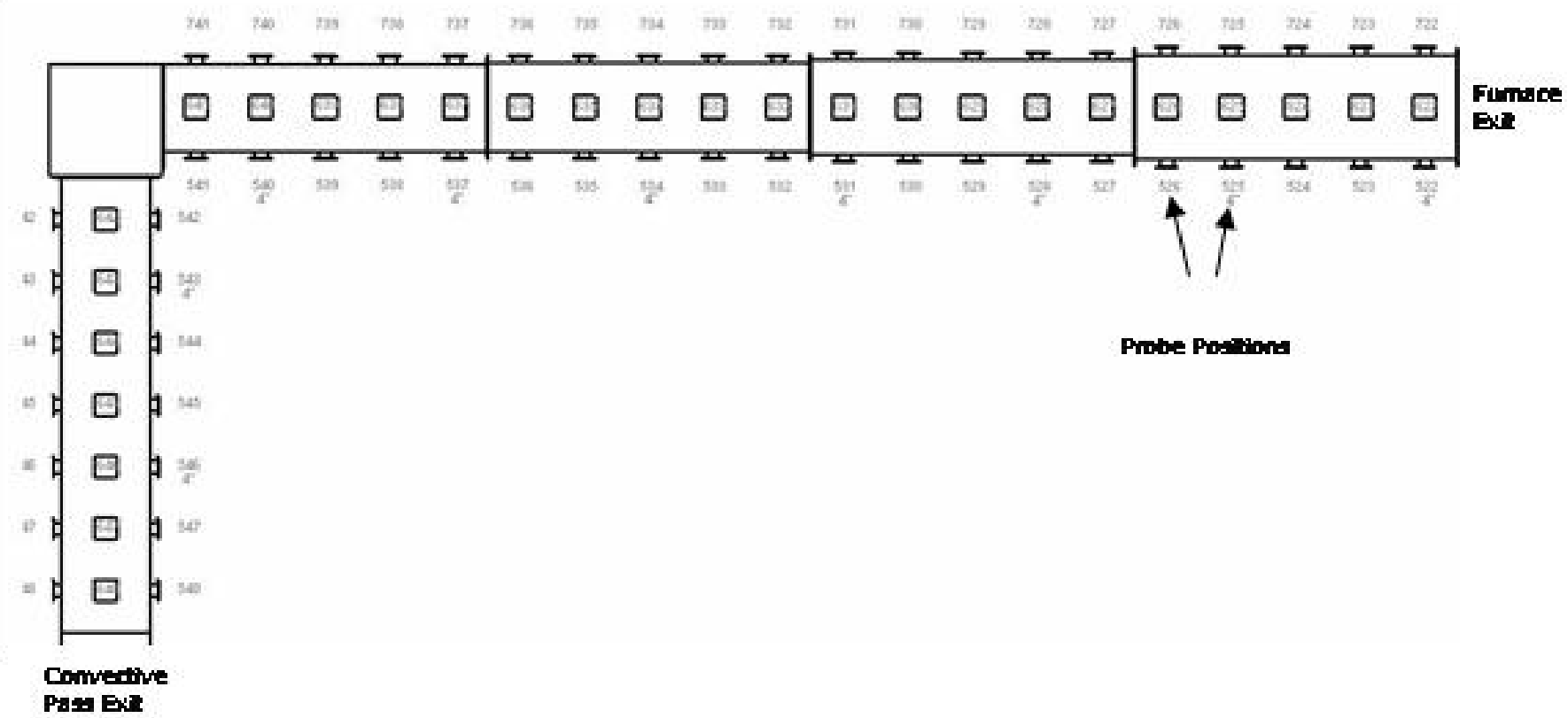

FIGURE No.2 **SCHEMATIC PLAN VIEW SHOWING LAYOUT OF COMBUSTION TEST FACILITY CONVECTIVE PASS AND LOCATION OF SAMPLING PORTS**

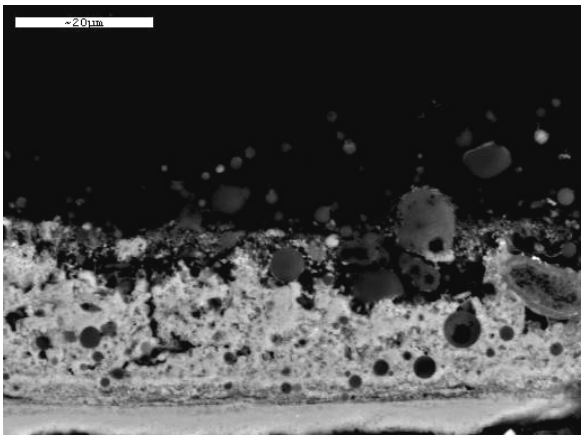

Back Scattered Electron Image

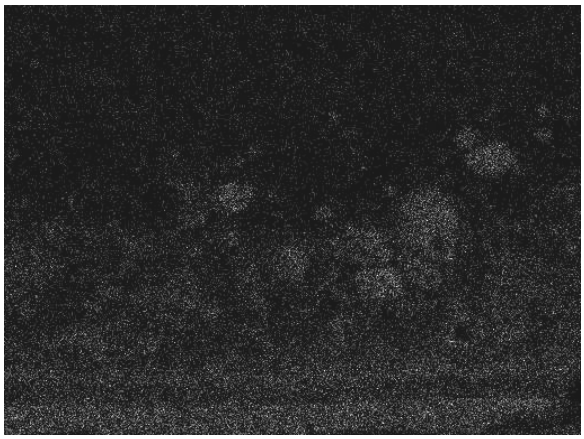

Oxygen X-ray Map

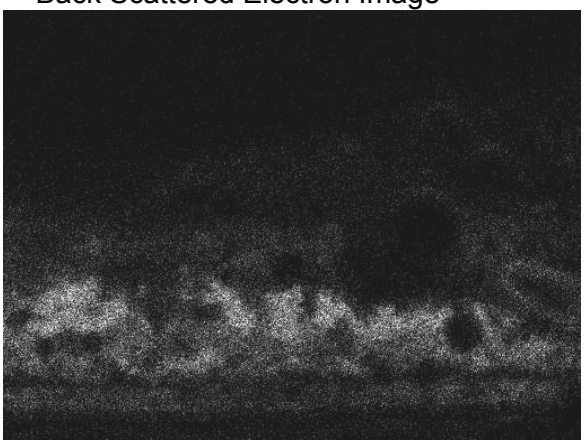

Sulphur X-ray Map

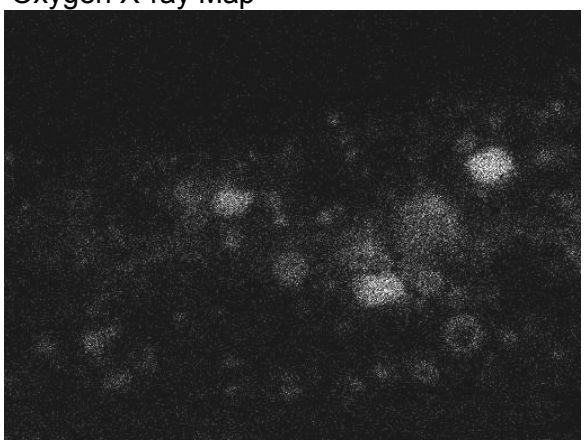

Silicon X-ray Map

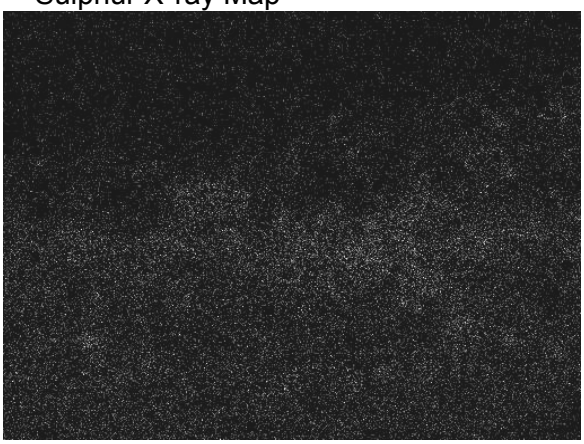

Potassium X-ray Map

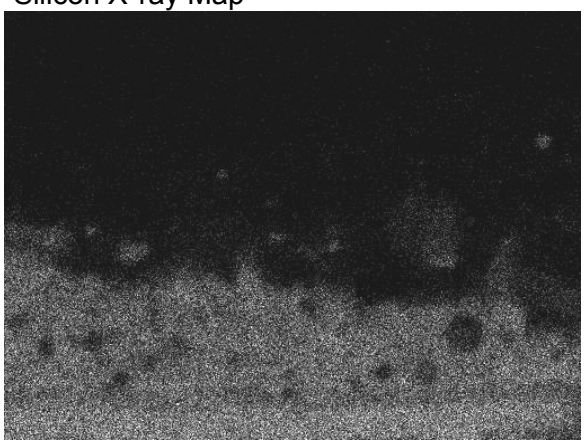

Iron X-ray Map

FIGURE No.5 **PLAIN CARBON STEEL SPECIMEN EXPOSED AT 475°C, 20% WOOD, RETAINING PARTICULATE ASH**

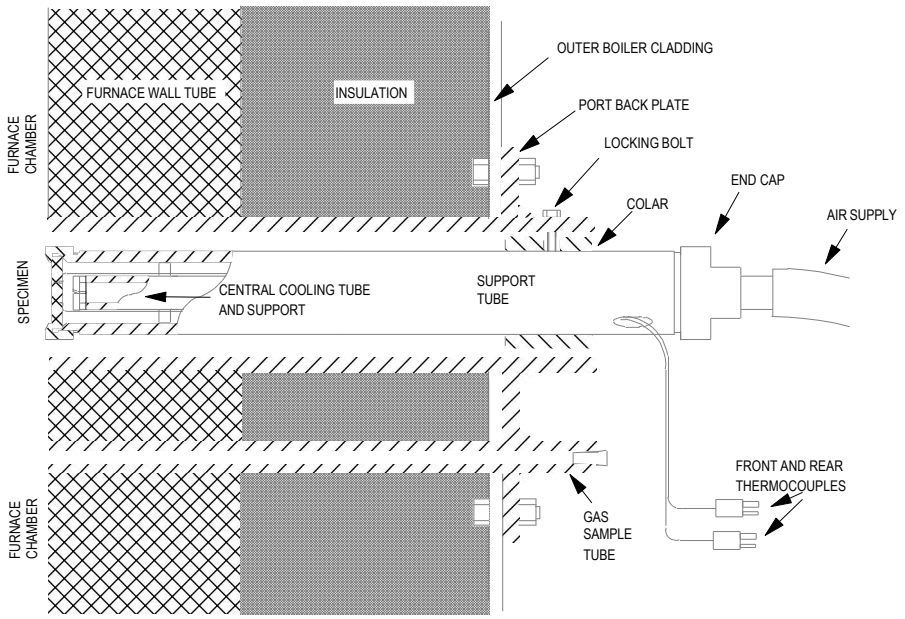

FIGURE No.3 **SCHEMATIC DIAGRAM SHOWING FURNACE WALL CORROSION PROBE AS EXPOSED IN THE CTF**

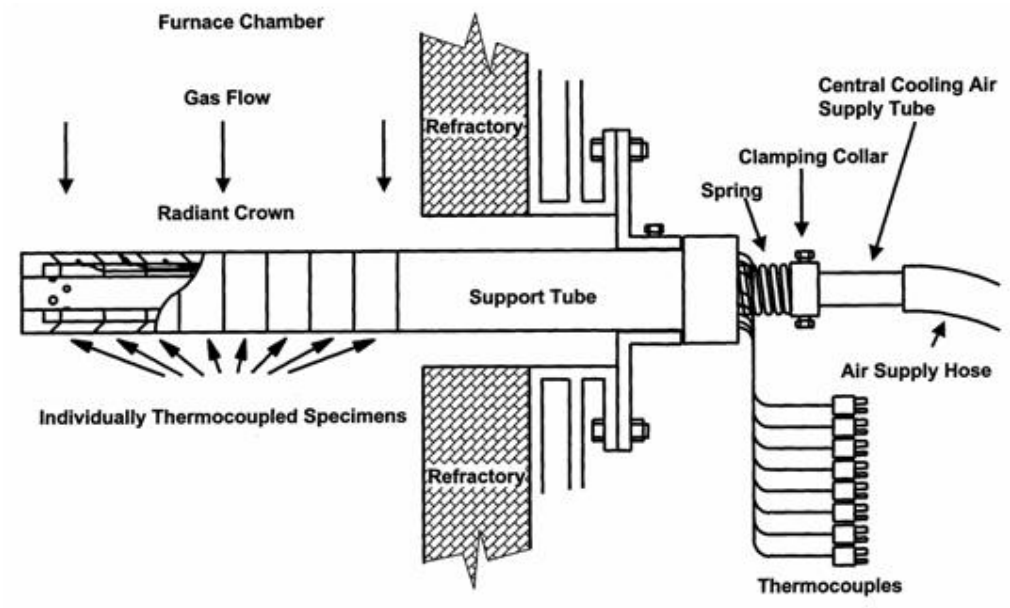

FIGURE No.4 **SCHEMATIC DIAGRAM SHOWING SUPERHEATER / REHEATER CORROSION PROBE AS EXPOSED IN THE CTF**

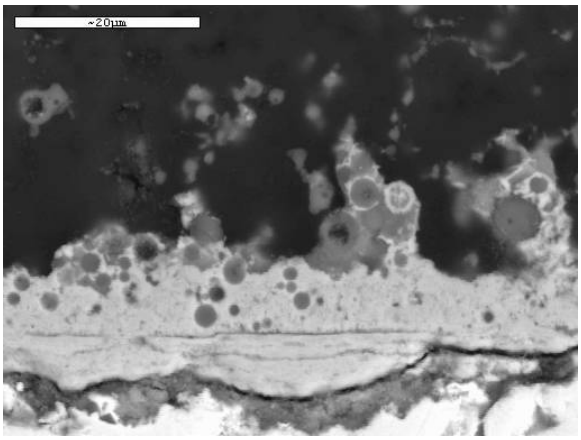

Back Scattered Electron Image

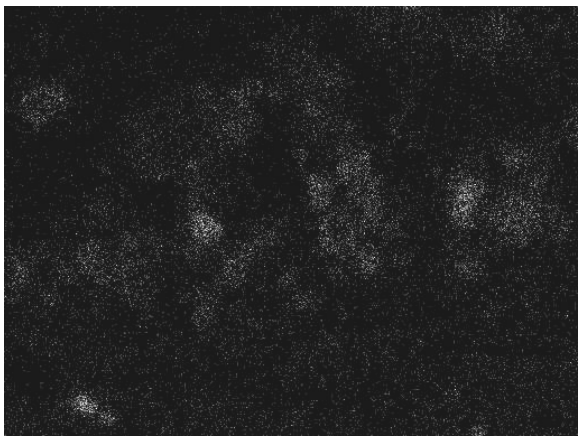

Silicon X-ray Map

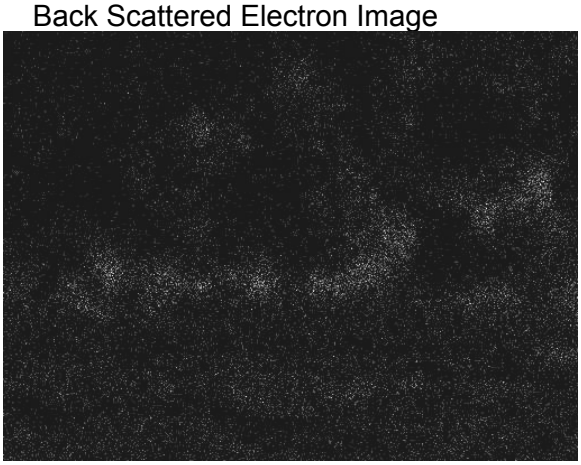

Sulphur X-ray Map

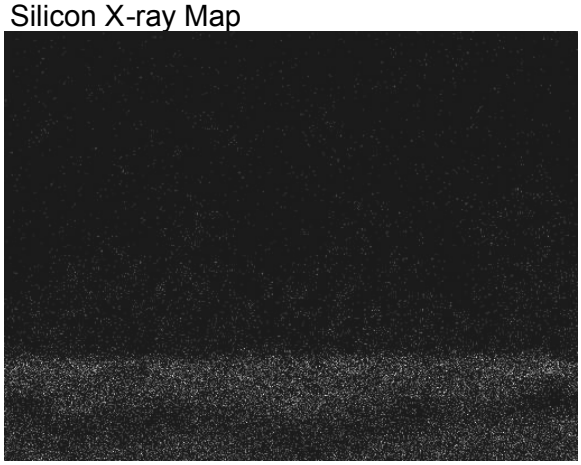

Chromium X-ray Map

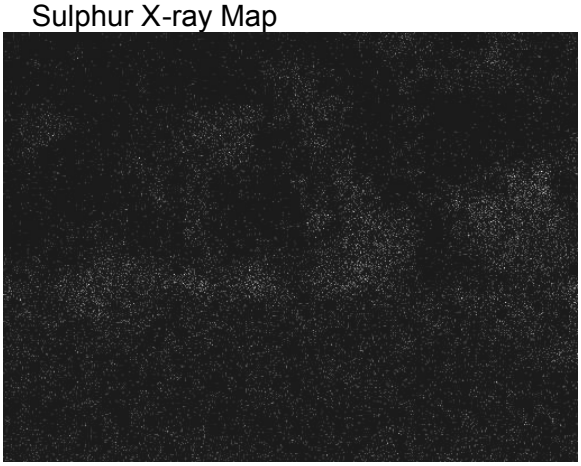

Potassium X-ray Map

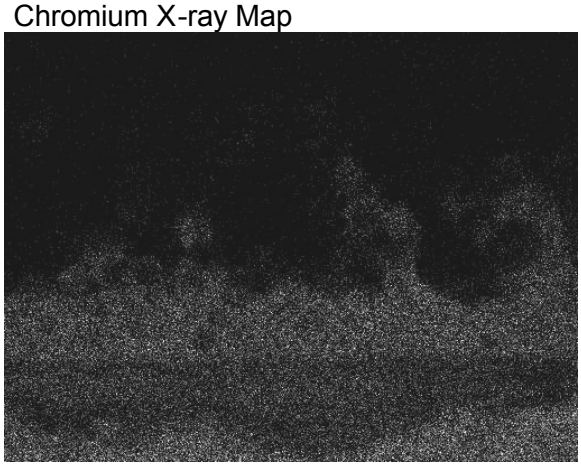

Iron X-ray Map

FIGURE No.6 **HCM12 SPECIMEN EXPOSED AT 574°C, 20% WOOD, RETAINING PARTICULATE AND AMORPHOUS ASH**

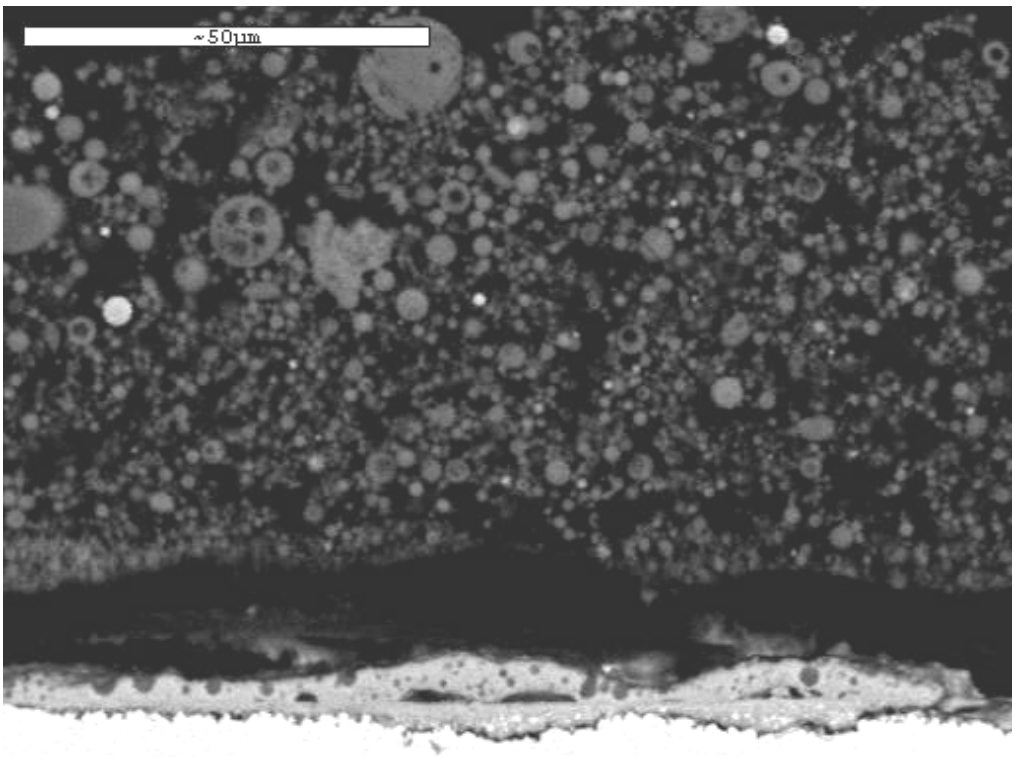

FIGURE No.7 **TP316 SUPERHEATER SPECIMEN 7 EXPOSED AT ~ 674°C, 20% WOOD, EXHIBITING THIN, DUPLEX CORROSION SCALE & PARTICULATE ASH**

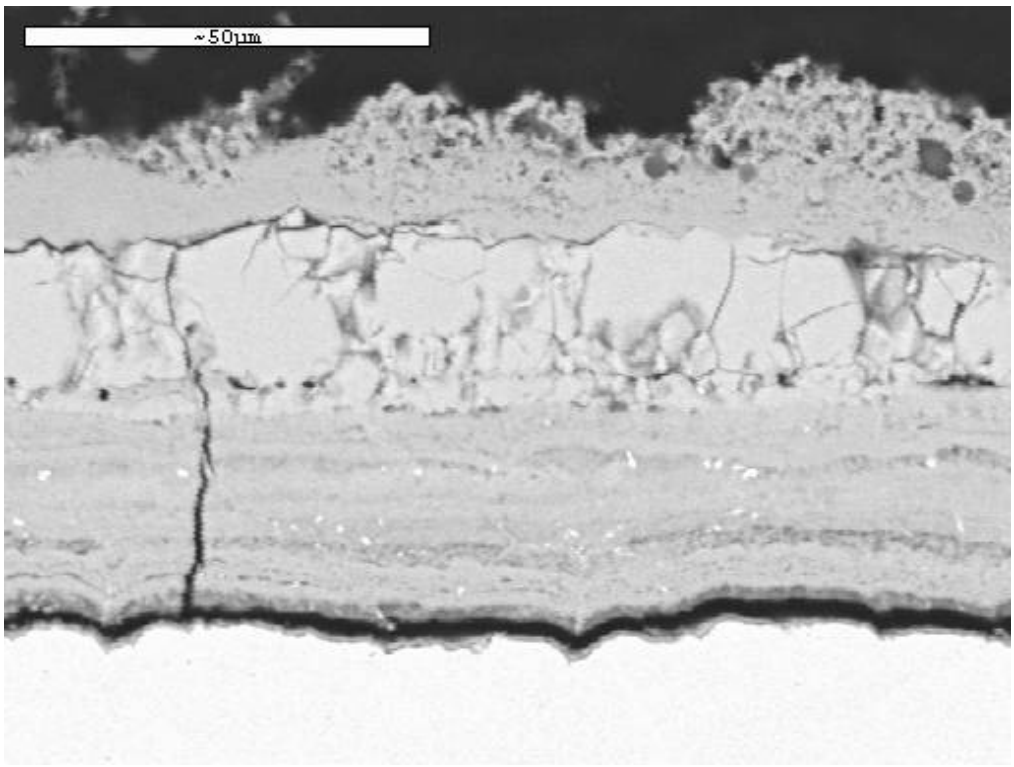

FIGURE No.8 **HCM2S SPECIMEN EXPOSED AT 550°C, 20%CCP, EXHIBITING DARK PHASE AT SCALE METAL INTERFACE (NOTE BLACK LINE IS DISBOND)**

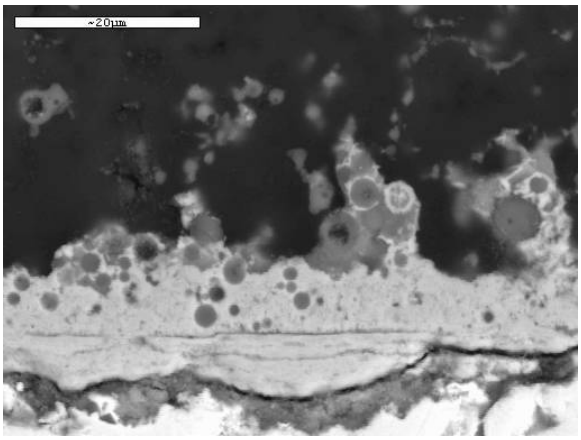

Back Scattered Electron Image

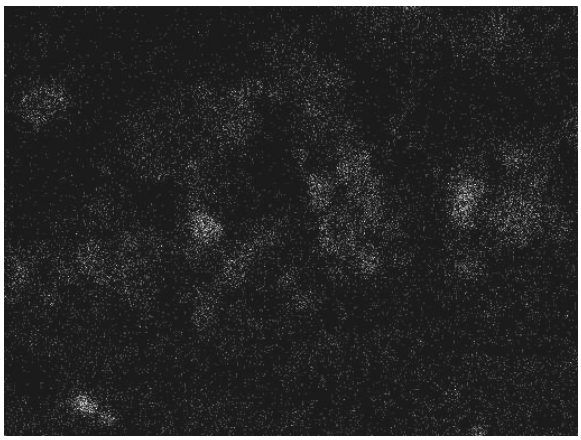

Silicon X-ray Map

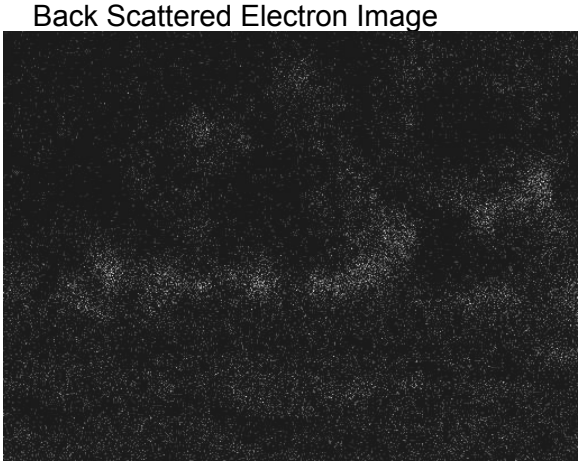

Sulphur X-ray Map

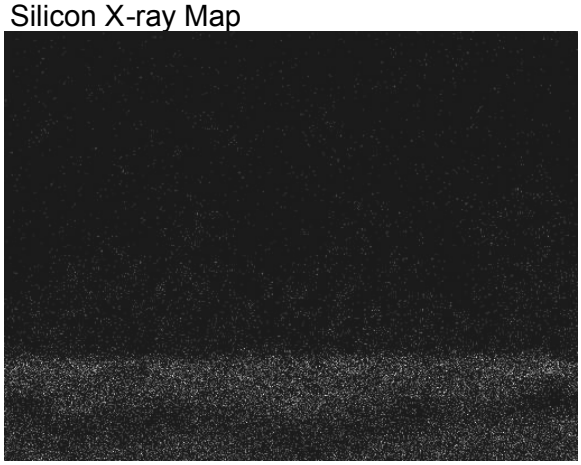

Chromium X-ray Map

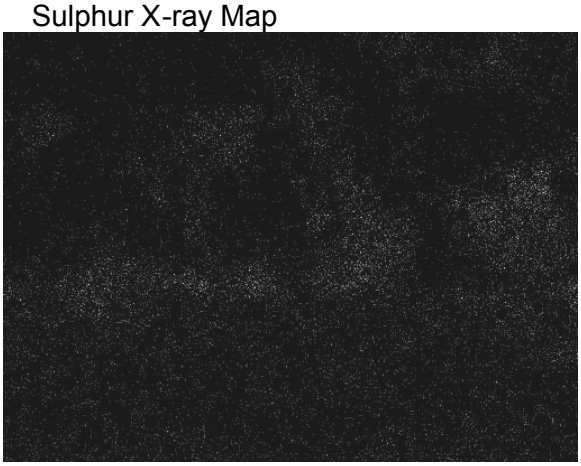

Potassium X-ray Map

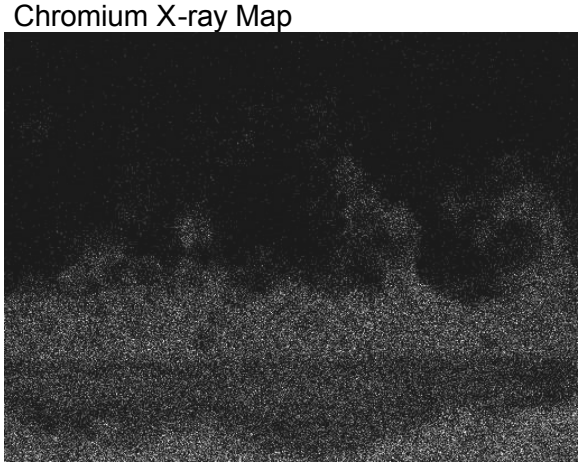

Iron X-ray Map

FIGURE No.6 **HCM12 SPECIMEN EXPOSED AT 574°C, 20% WOOD, RETAINING PARTICULATE AND AMORPHOUS ASH**

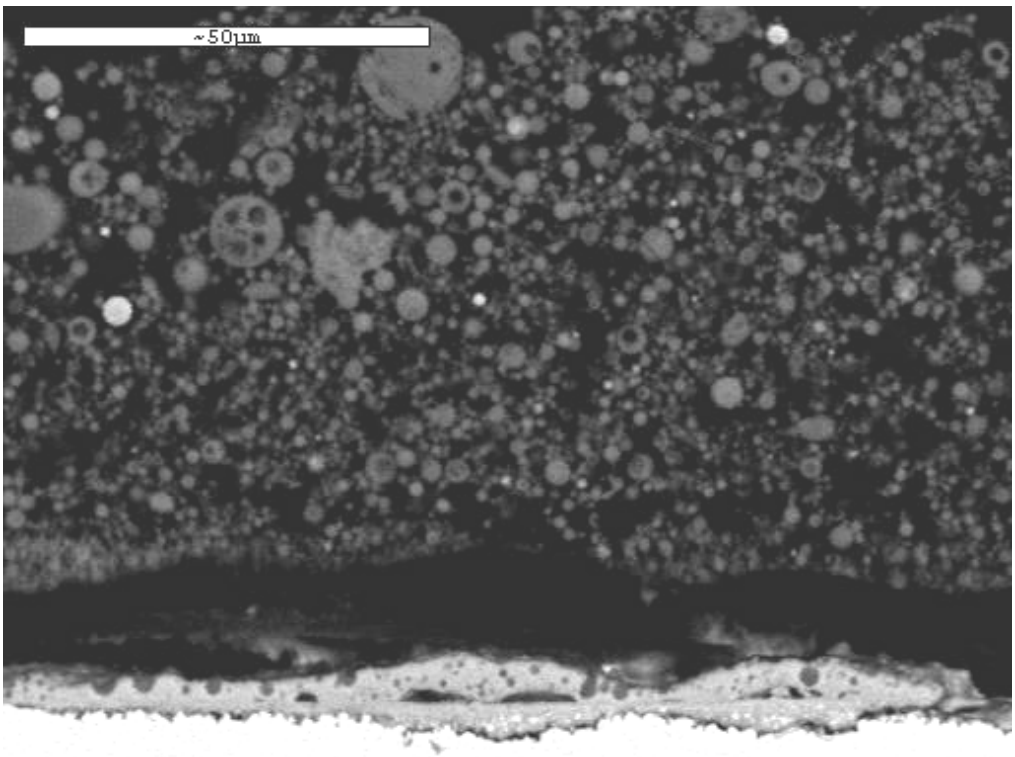

FIGURE No.7 **TP316 SUPERHEATER SPECIMEN 7 EXPOSED AT ~ 674°C, 20% WOOD, EXHIBITING THIN, DUPLEX CORROSION SCALE & PARTICULATE ASH**

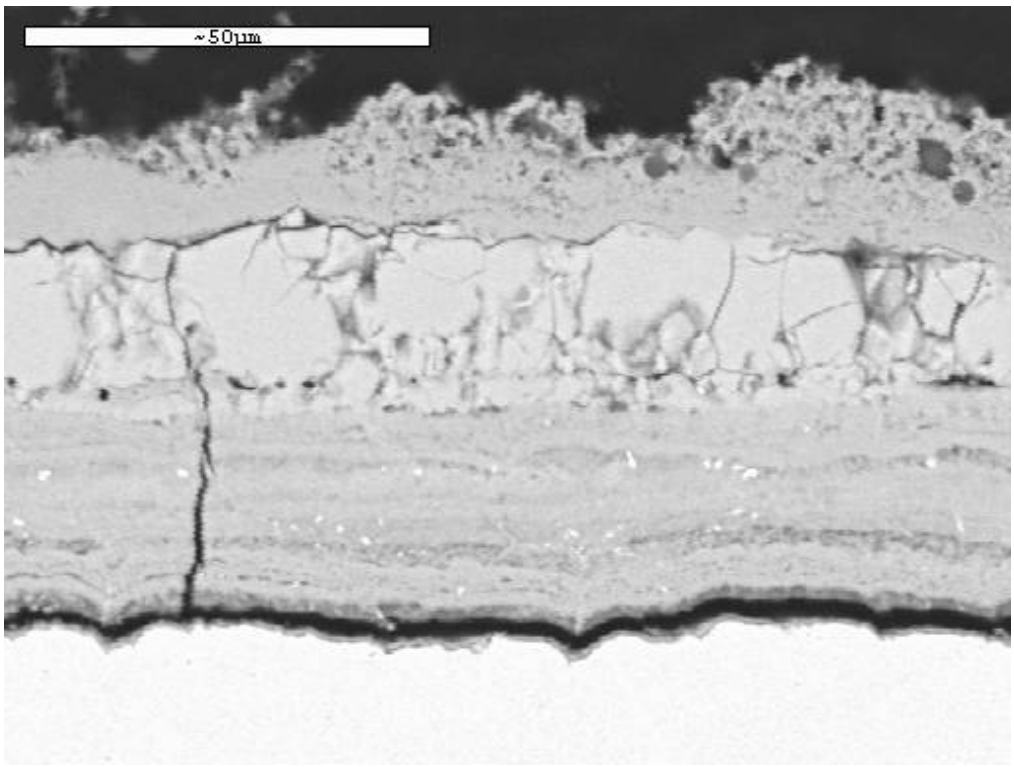

FIGURE No.8 **HCM2S SPECIMEN EXPOSED AT 550°C, 20%CCP, EXHIBITING DARK PHASE AT SCALE METAL INTERFACE (NOTE BLACK LINE IS DISBOND)**